







Outline

- RR Lyrae Stars (+ Anomalous cepheids)
 - star formation history tracers
 - metallicity tracers
 - distance tracers
 - population tracers
- The Local Group
 - a changing scenario
 - the impact of surveys

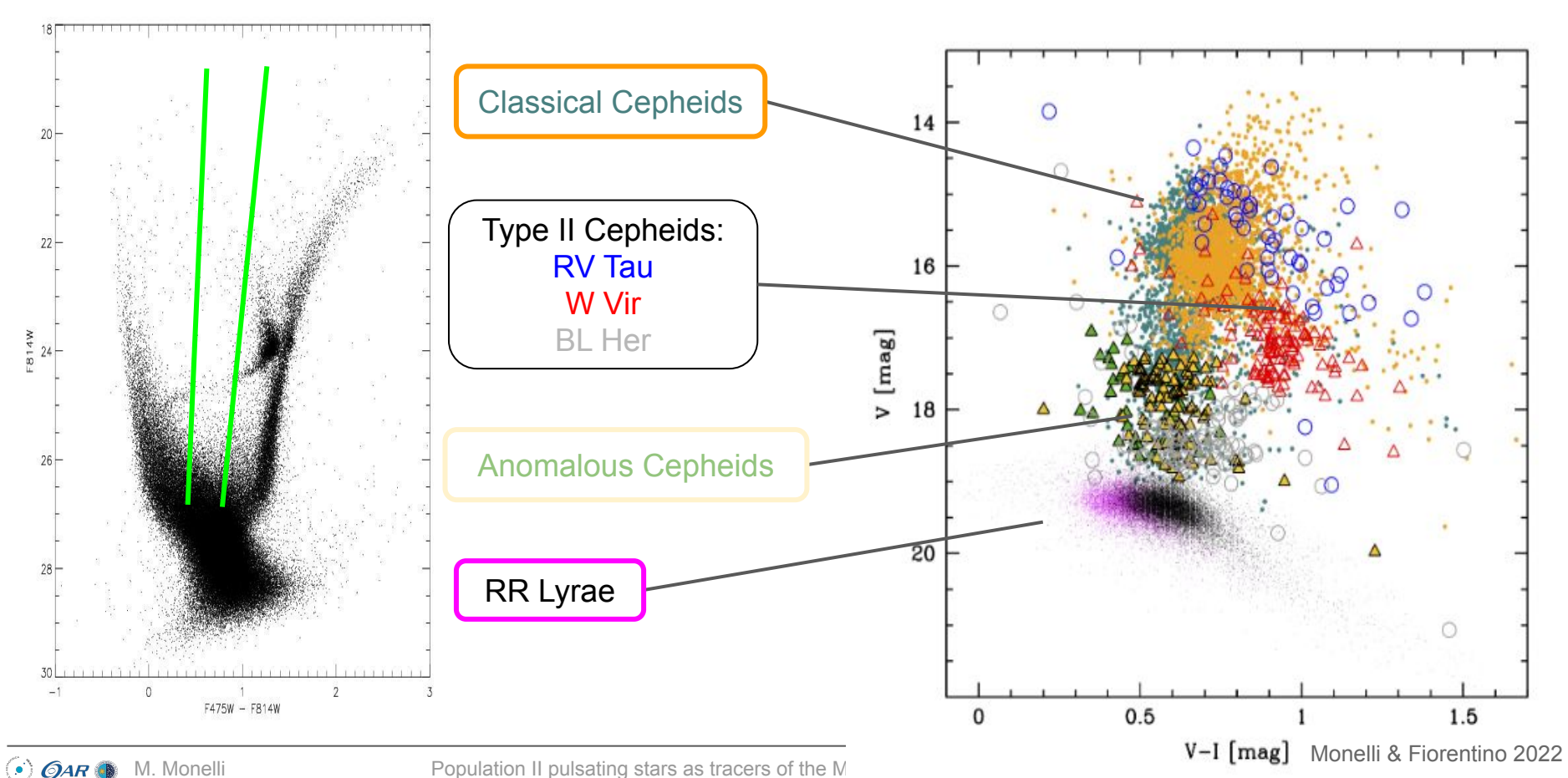
Take-home message

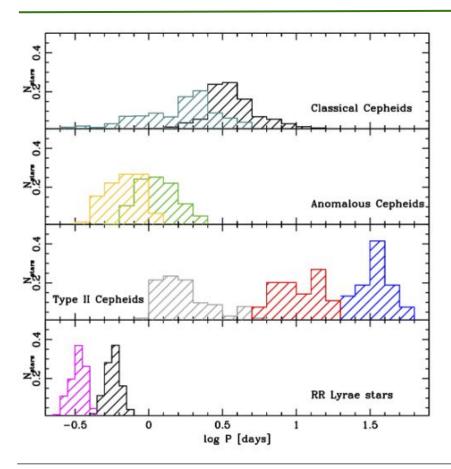


You will be drowning in data!



RR Lyrae stars





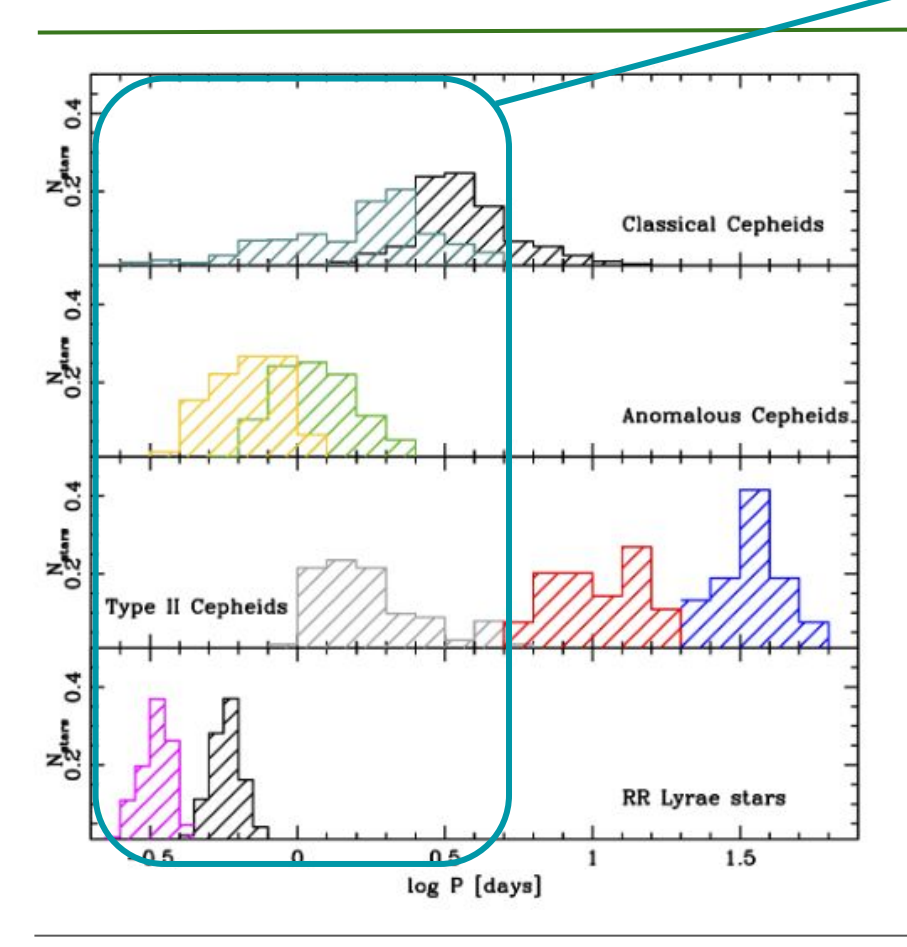
Classical Cepheids 0.5 - > 150 d

Anomalous Cepheids 0.5 - 2.5 d

Type II Cepheids BL Her: P < 4 dW Vir: 4 < P < 20 dRV Tau: P > 20 d

RR Lyrae 0.2 - 1.0 d

Monelli & Fiorentino 2022



Classical Cepheids 0.5 - > 150 d

Anomalous Cepheids 0.5 - 2.5 d

Type II Cepheids

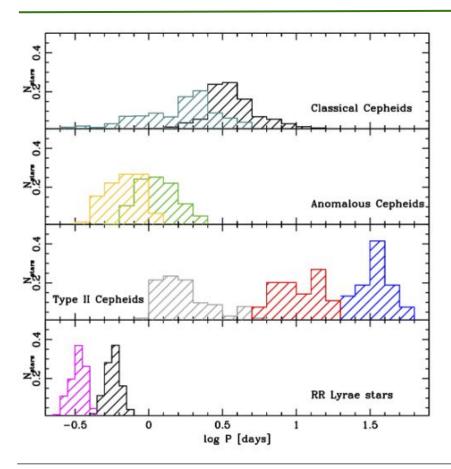
BL Her: P < 4 d post-(blue)HB

W Vir: 4 < P < 20 d AGB

RV Tau: P > 20 d post-AGB

RR Lyrae 0.2 - 1.0 d

Monelli & Fiorentino 2022



Classical Cepheids 0.5 - > 150 d

Anomalous Cepheids 0.5 - 2.5 d

INTERMEDIATE-AGE 1-6 Gyr OLD > 10 Gyr

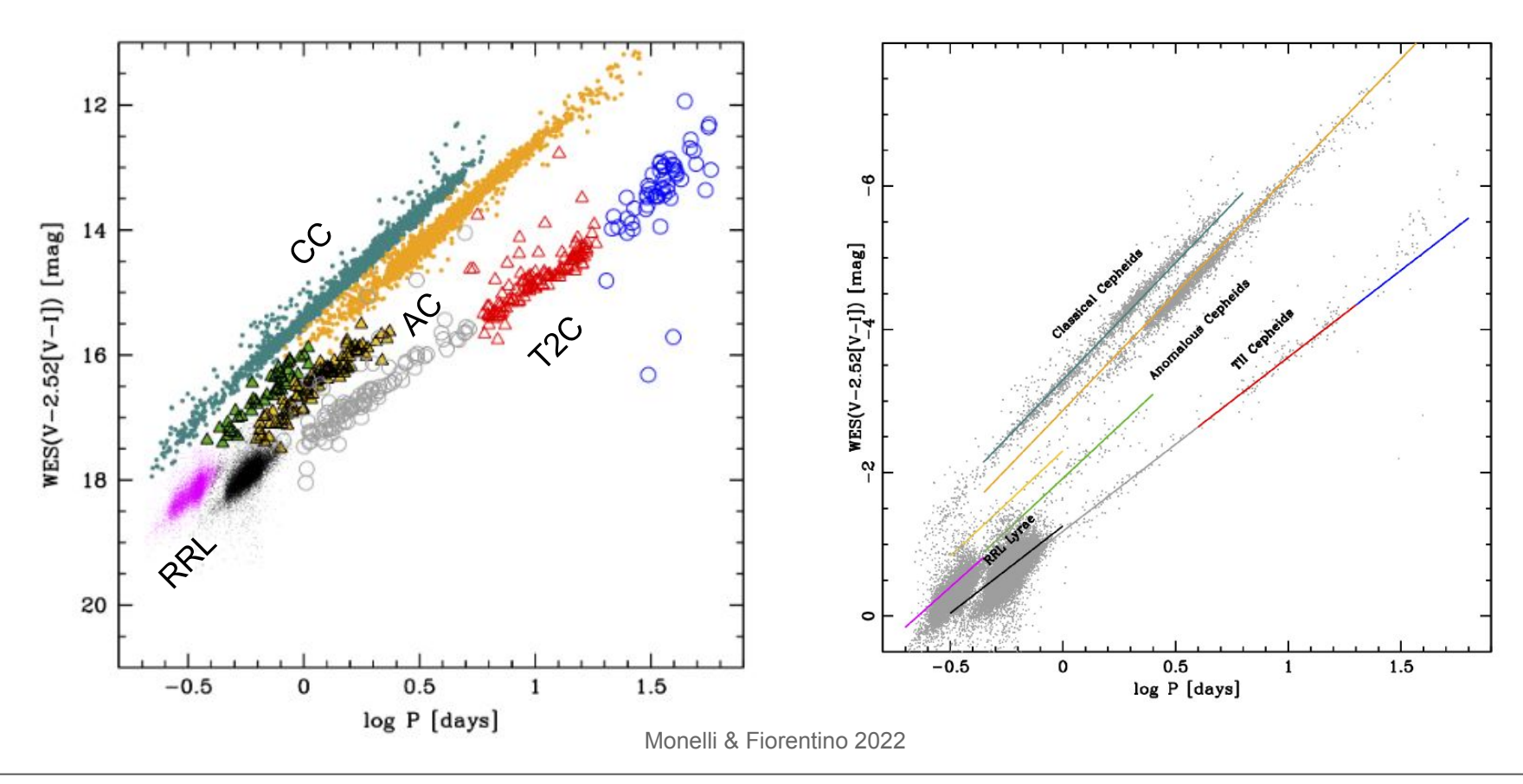
Type II Cepheids
BL Her: P < 4 d
W Vir: 4 < P < 20 d

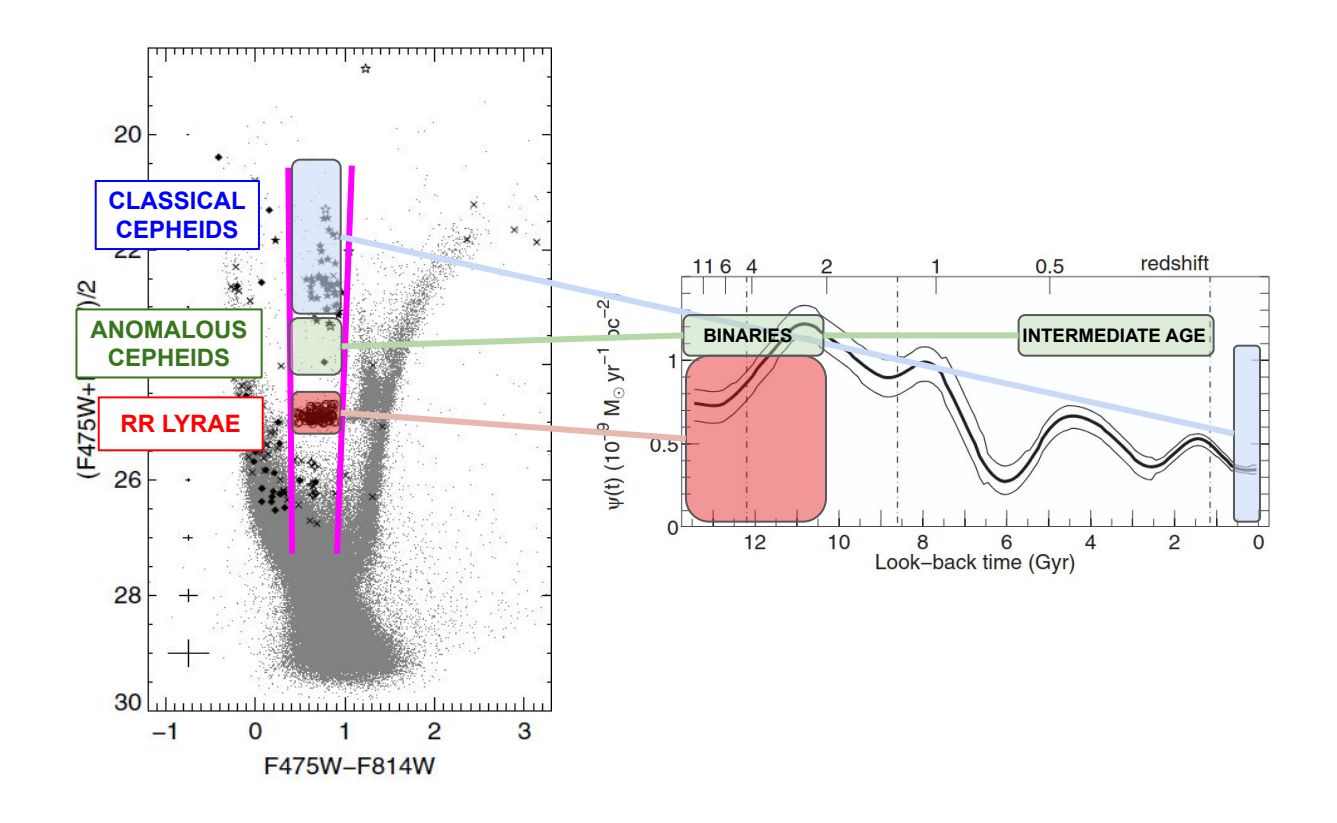
RV Tau: P > 20 d

OLD > 10 Gyr M < 1 M_☉

RR Lyrae 0.2 - 1.0 d

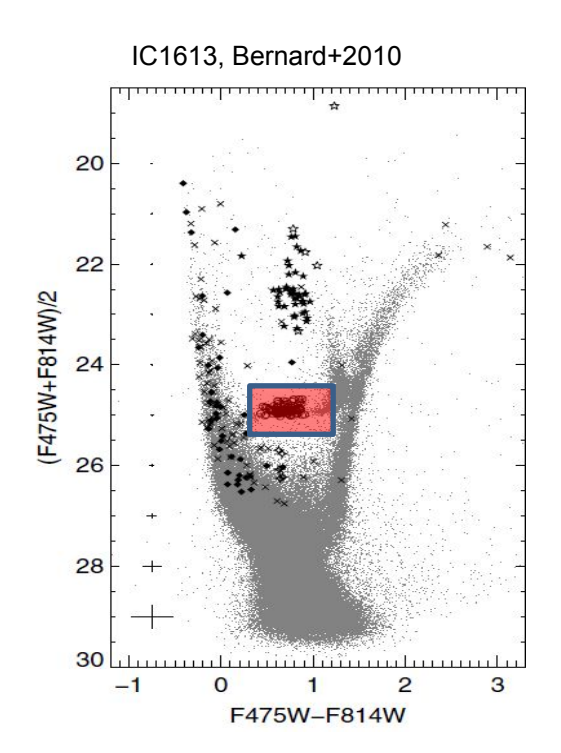
Monelli & Fiorentino 2022





RR Lyrae as:

- ★ tracers of the old population
 - → Milky Way
 - → Local Group (dwarf) galaxies
- ★ tracers of metallicity and chemical evolution and chemical gradients
- ★ fundamental distance indicators



RR Lyrae

Best old pop. tracers (> 10 Gyr)

→ halo, thick disc, dwarfs, GCs

Low-mass (\sim 0.6-0.8M $_{\odot}$) HB stars

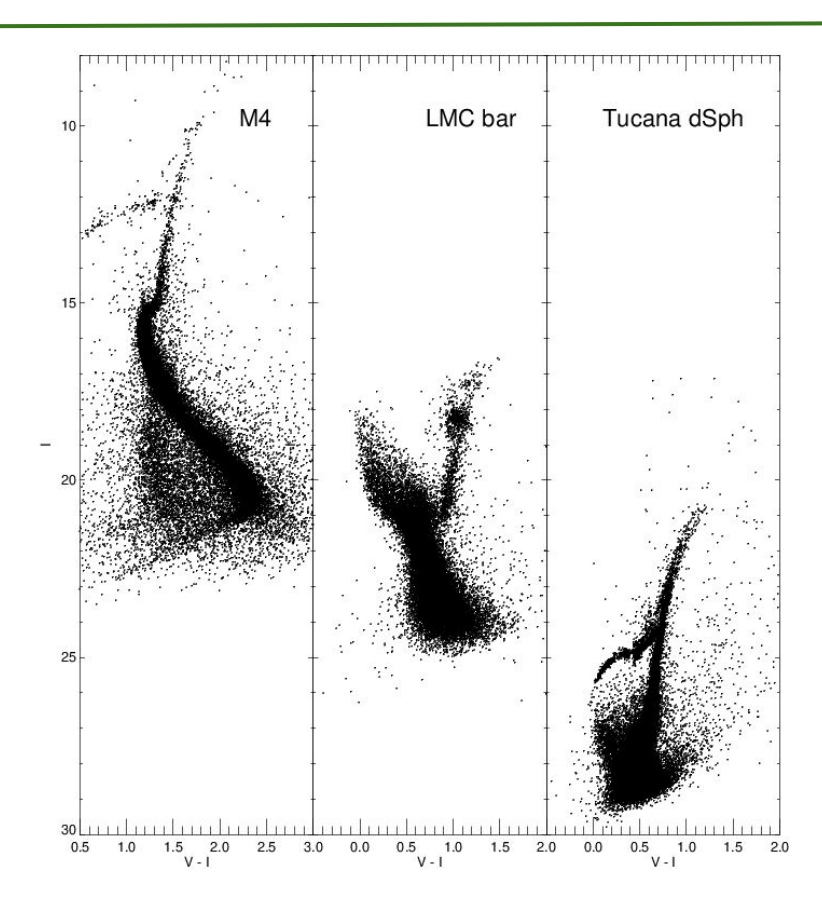
P ~ 0.25 to 1 d

Amplitude(V) ~ 0.3 to 1.5 mag

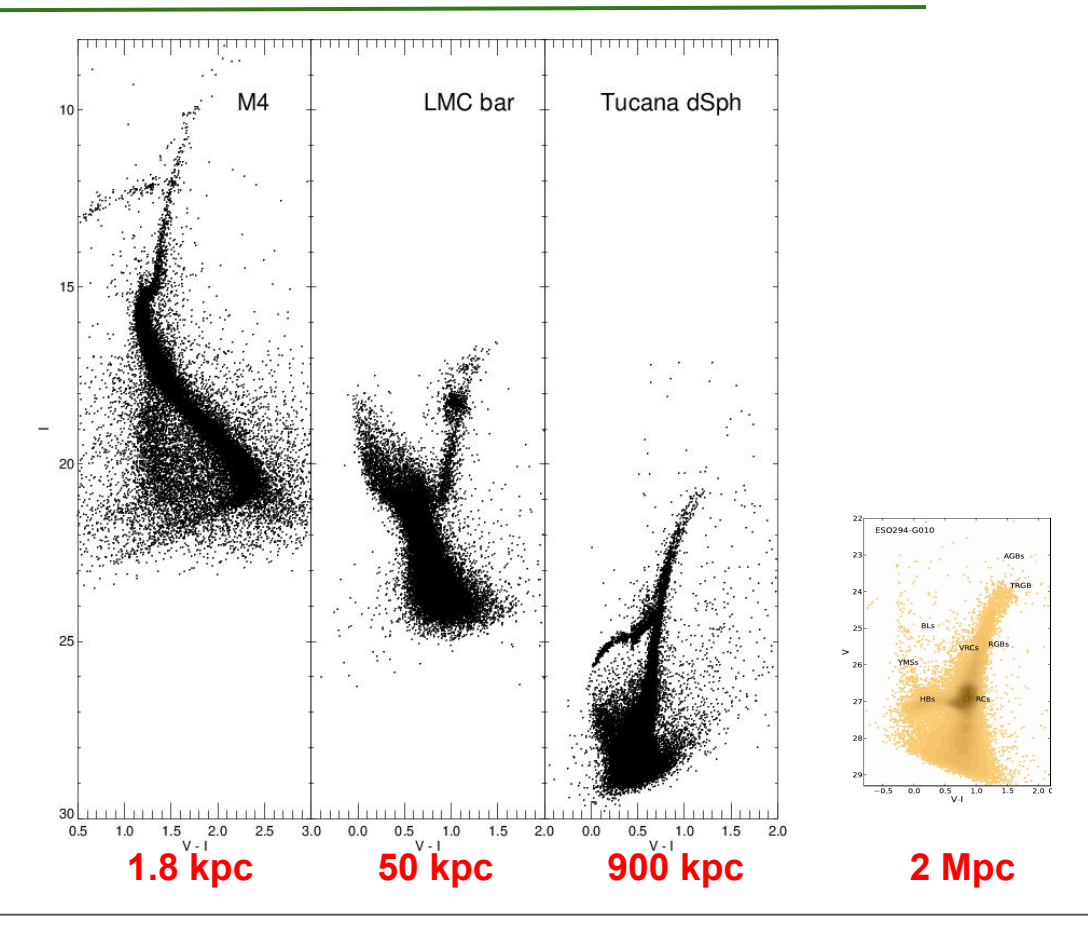
Intrinsically bright $(M_{V} \sim 0.5)$

Fundamental distance indicators

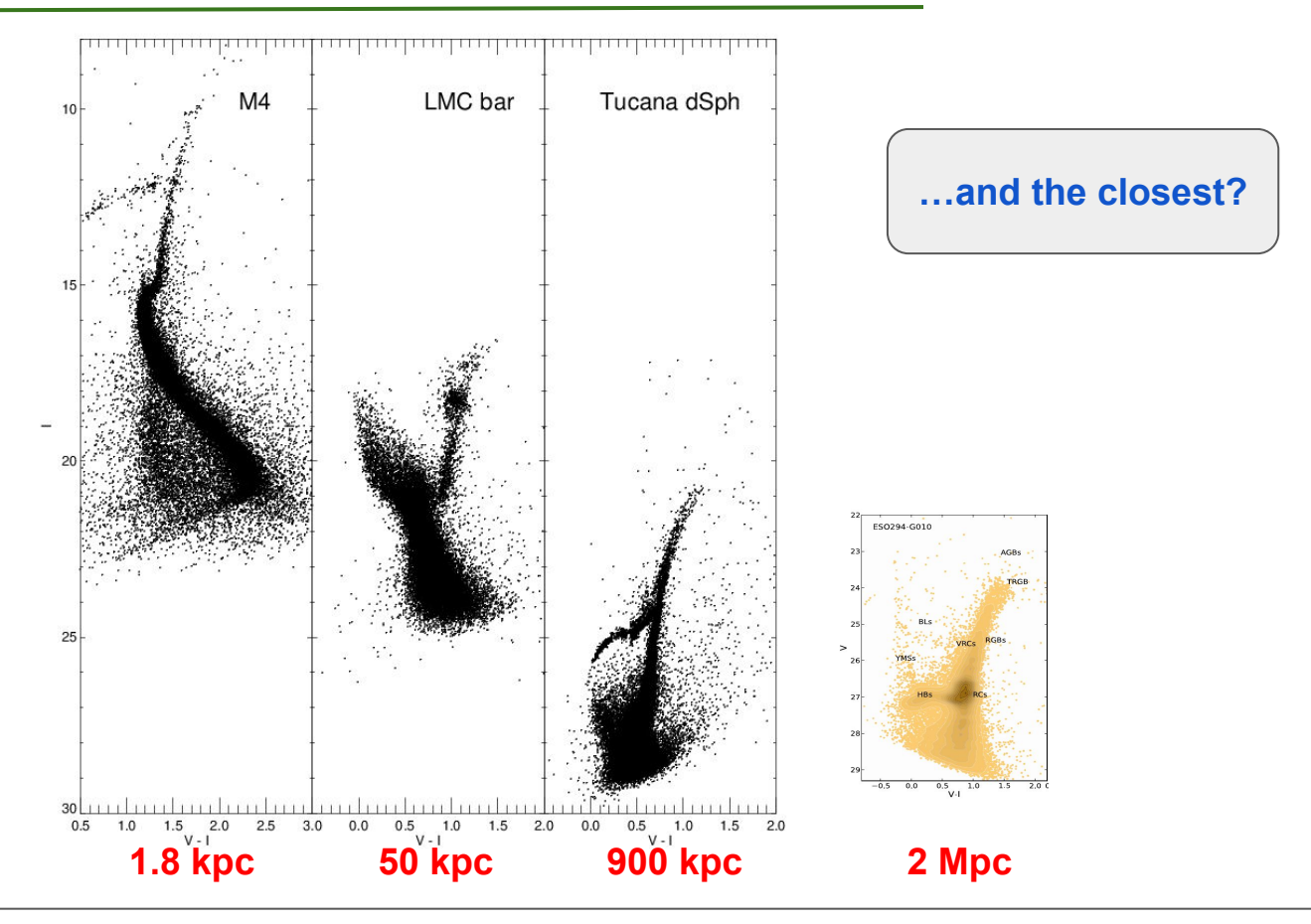
How far is the most distant known RRL star?



How far is the most distant known RRL star?



How far is the most distant known RRL star?



How many RRL stars do we know?



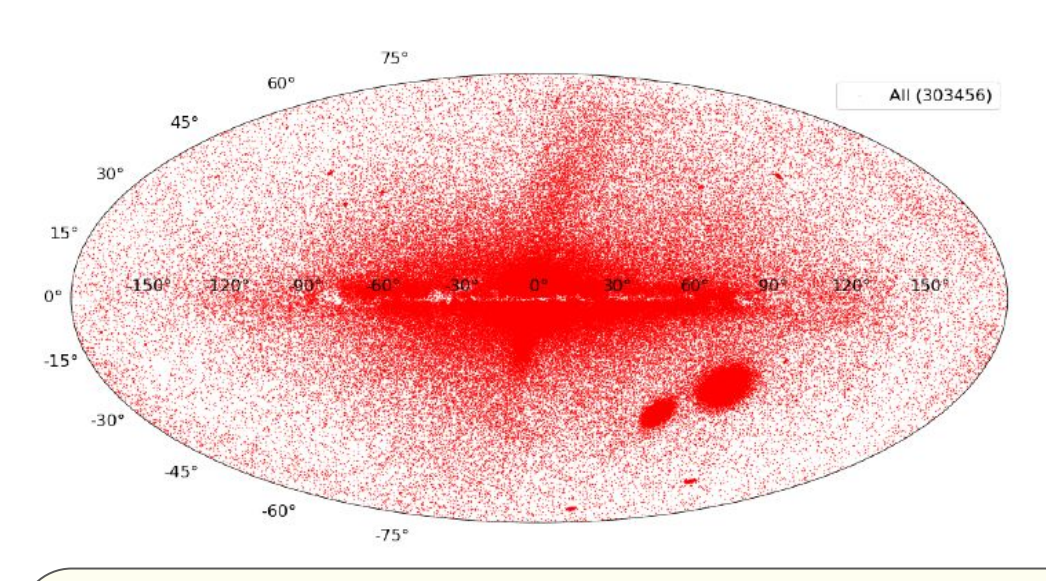
How many RRL stars do we know?

| OGLE | 2002- | 129,000 | VI |
|------------|-----------------|---------|-----------------------------------|
| PAN-STARRS | DR2 (3 yr) | 45,000 | griz |
| ASAS-SN | 2013- | 36,000 | VI - g |
| ZTF | DR3 (21 months) | 70,000 | gri |
| Gaia | DR3 (34 months) | 270,000 | G G _{BP} G _{RP} |

Full credit for the next slides to Vittorio Braga and Giuseppe Bono

Photometric catalogue

Bono, Braga+ subm.



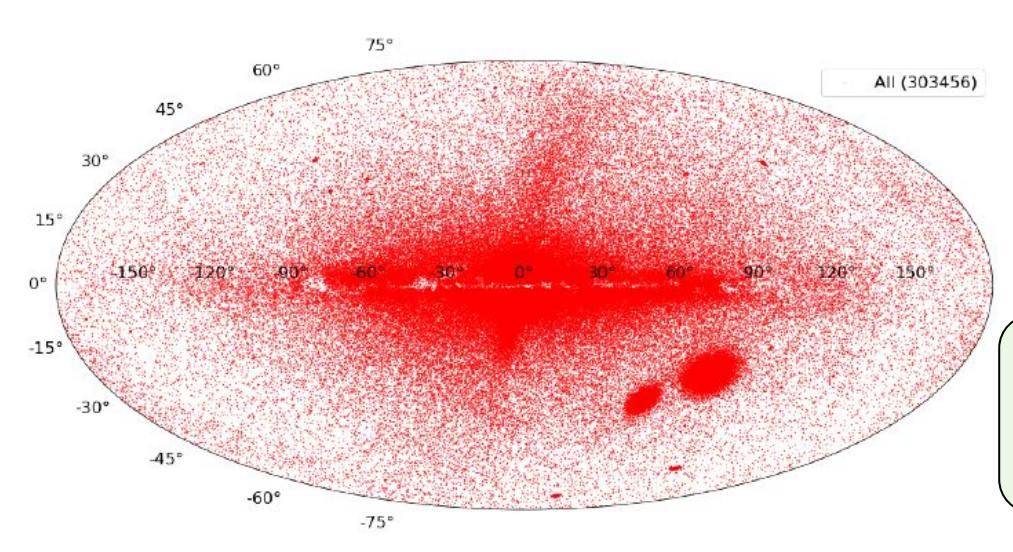
Gaia

optical - Catalina, ASAS, ASAS-SN, GCVS, SDSS, OGLE, Pan-STARRS1, LINEAR, ROTSE-I, LONEOS, ZTF, QUEST, near infrared - 2MASS, UKIRT, VHS mid infrared - WISE, NEO-WISE, AllWISE, SPITZER ultraviolet - GALEX

Photometric catalogue

75364

0.06



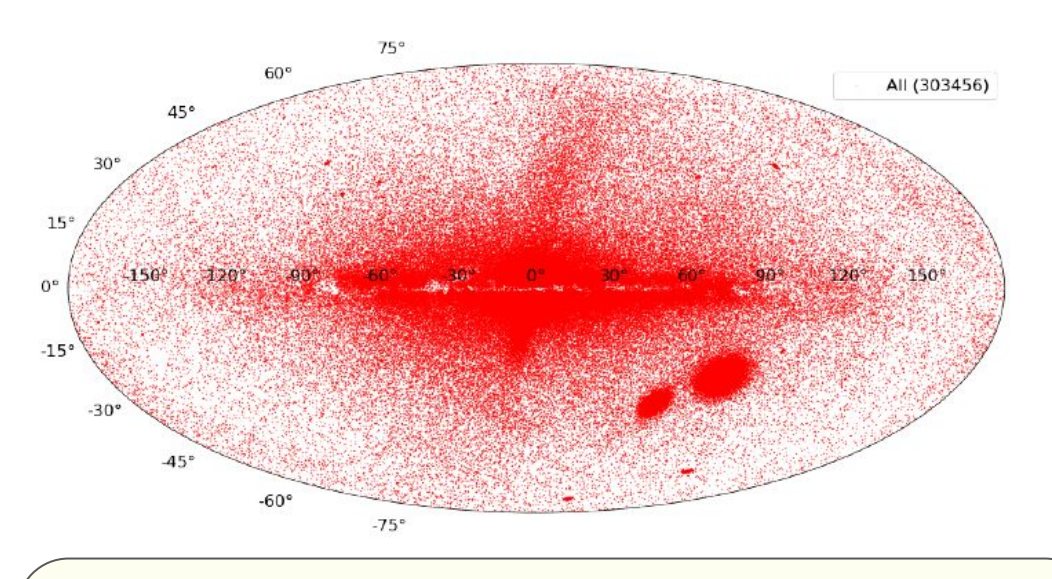
7.62 < G < 21.19 mag 4.35 < K < 19.31 mag 5.94 < W1 < 19 mag 12.5 < NUV < 23.2 mag

0.04 0.03 ≥ 0.02 0.01 0.00 12 0.08 139053 0.07 € 0.06 S 0.05 .º 0.04 0.03 0.02 0.01 10 281243 S 0.06 E 0.04 0.02 0.00 12 16

Gaia

optical - Catalina, ASAS, ASAS-SN, GCVS, SDSS, OGLE, Pan-STARRS1, LINEAR, ROTSE-I, LONEOS, ZTF, QUEST, near infrared - 2MASS, UKIRT, VHS mid infrared - WISE, NEO-WISE, AllWISE, SPITZER ultraviolet - GALEX

Photometric catalogue



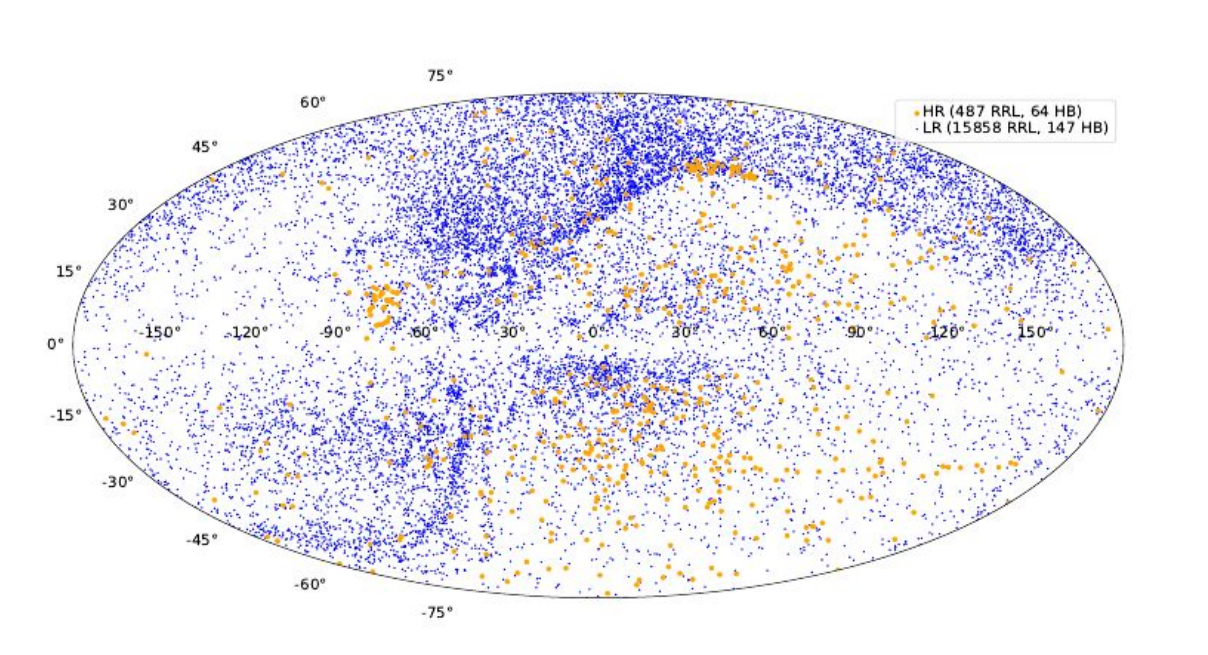
RRab (200177) 10000 RRc (98888) RRd (4391) 8000 6000 Counts 4000 2000 0.2 0.3 0.4 0.5 0.6 0.7 0.9 1.0 Period [d]

Gaia

optical - Catalina, ASAS, ASAS-SN, GCVS, SDSS, OGLE, Pan-STARRS1, LINEAR, ROTSE-I, LONEOS, ZTF, QUEST, near infrared - 2MASS, UKIRT, VHS mid infrared - WISE, NEO-WISE, AllWISE, SPITZER ultraviolet - GALEX

M. Monelli

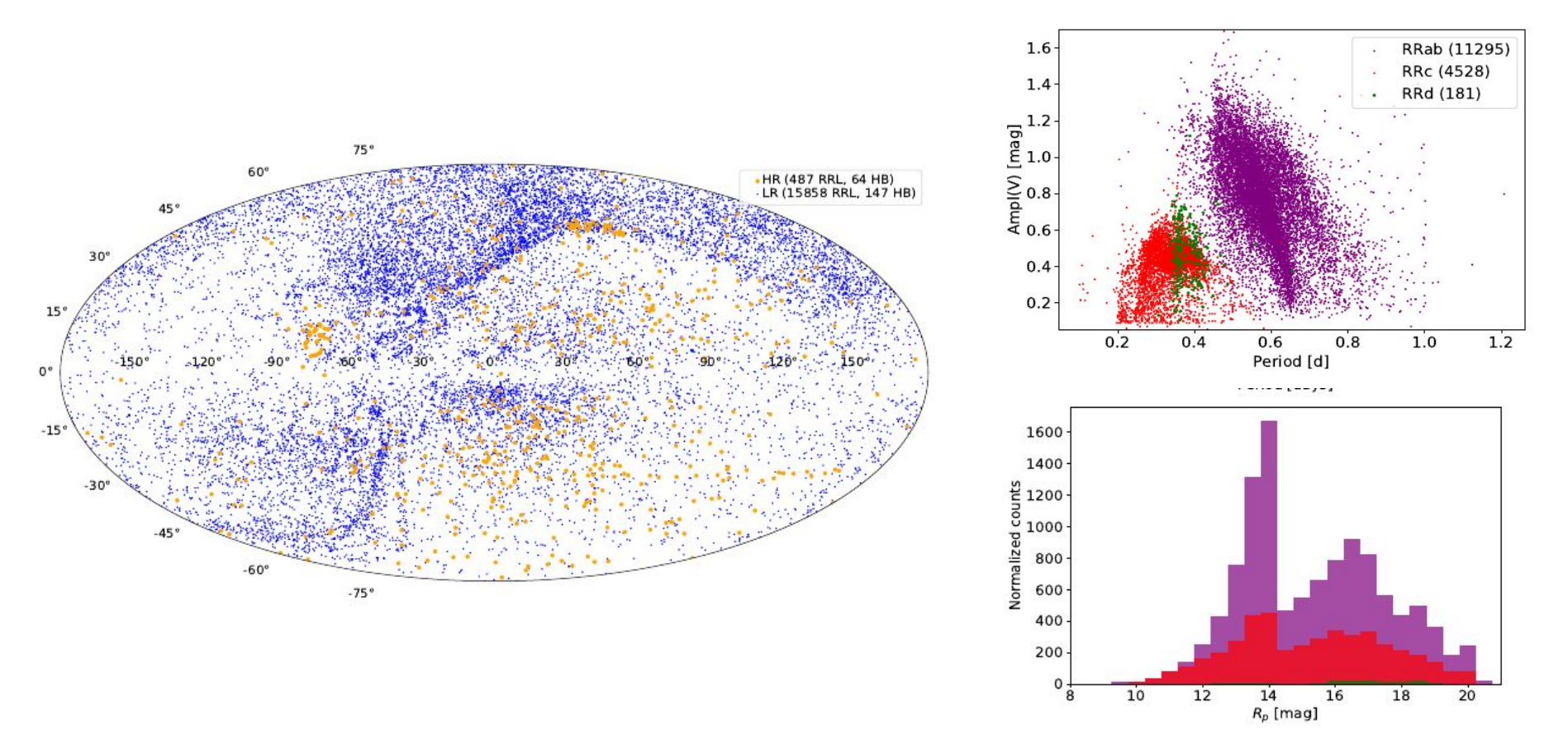
Spectroscopic catalogue



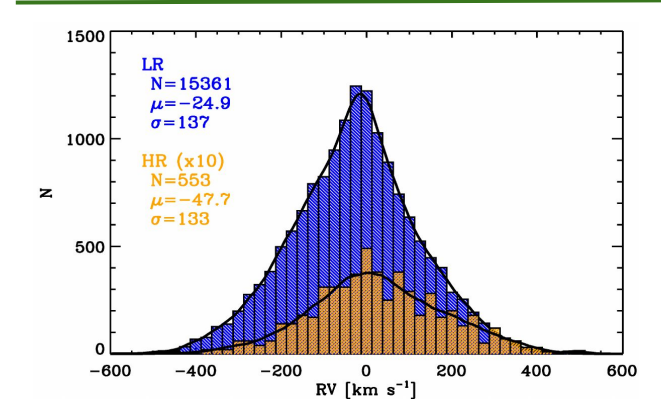
| Dataset | RV | | [Fe/H] | | $[\alpha/\mathrm{Fe}]$ |
|----------------------------|------|---------------|----------------|--------------------|------------------------|
| | LR | $_{ m HR}$ | LR | HR | HR |
| | —RF | RL— | | | |
| Crestani | | $576^{\rm a}$ | $8117^{\rm b}$ | $159 + 78^{\circ}$ | $201^{\rm d}$ |
| D24 | | | | 78 | 60 |
| D25 | | | | 3 | |
| Sesar et al. (2013) | | *** | 21 | *** | |
| Liu et al. (2020) | | | 303 | | |
| LAMOST | 5436 | | | | |
| SDSS | 1688 | | | * * * | |
| Gaia | 5895 | | | | |
| GALAH | | 2307 | | 119 | 51 |
| Zinn et al. (2020) | 104 | | 195 | | |
| Kinman et al. (2012) | | | 51 | | |
| Dambis et al. (2013, 2014) | | 0.55 | 9 | 10000 | |
| RAVE | | | 3 | | |
| Duffau et al. (2014) | | 39 | | 36 | |
| Hansen et al. (2011) | | 2 | | | |
| Nemec et al. (2013) | | 11 | | | |
| DESI | 1227 | | | | |
| G21 | | | | 14 | |
| Medina et al. (2021) | | 15 | | | |
| | —Н | В— | | | |
| For & Sneden (2010) | | 45 | | 46 | 39 |
| Kinman ^e | 123 | 18 | | 9 | 7 |

Total of ~16,000 stars

Spectroscopic catalogue



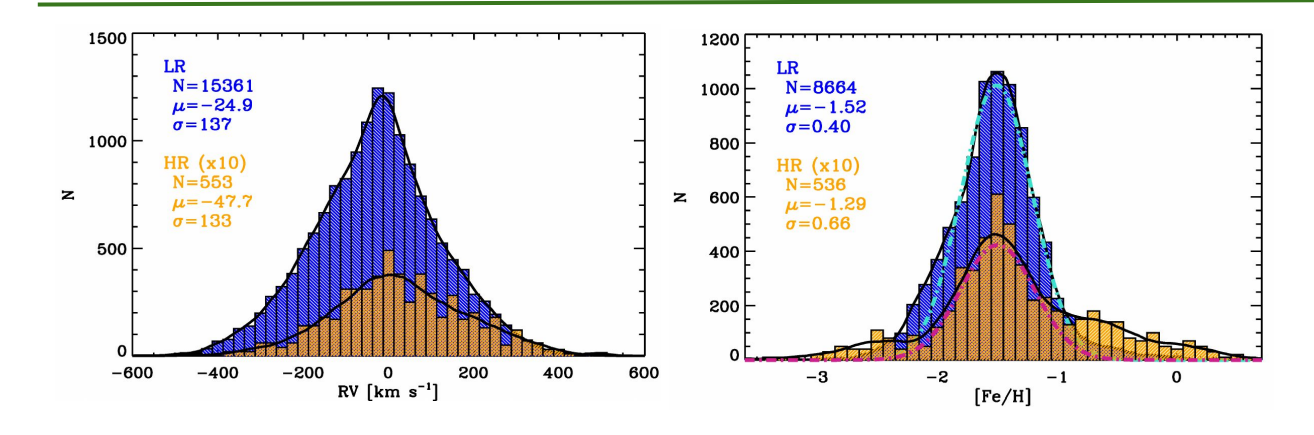
Spectroscopic catalogue



Radial velocity

- symmetric around 0
- HR and LR similar
- high velocity tails

Spectroscopic catalogue



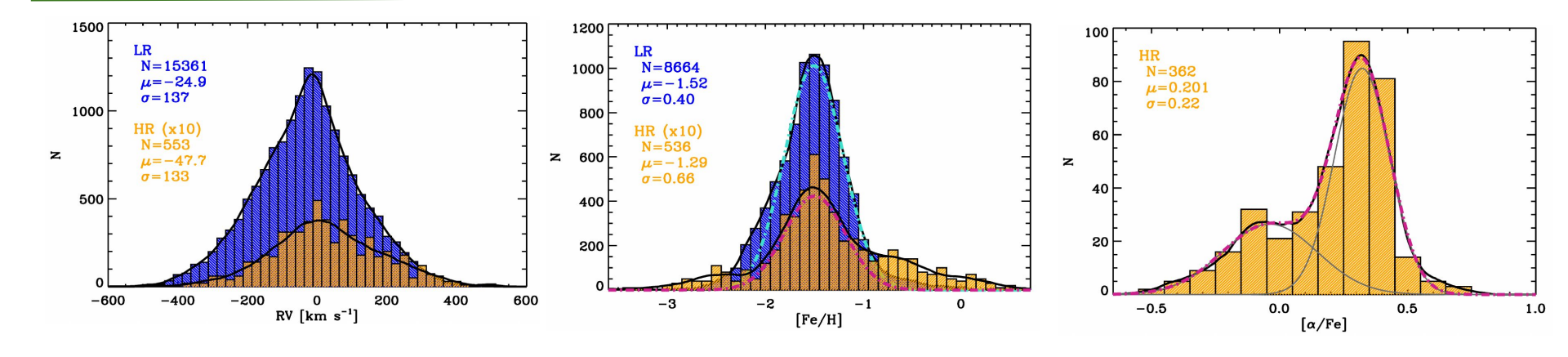
Radial velocity

- symmetric around 0
- HR and LR similar
- high velocity tails

Metallicity

- similar distribution (peak)
- tails biassed by the samples

Spectroscopic catalogue



Radial velocity

- symmetric around 0
- HR and LR similar
- high velocity tails

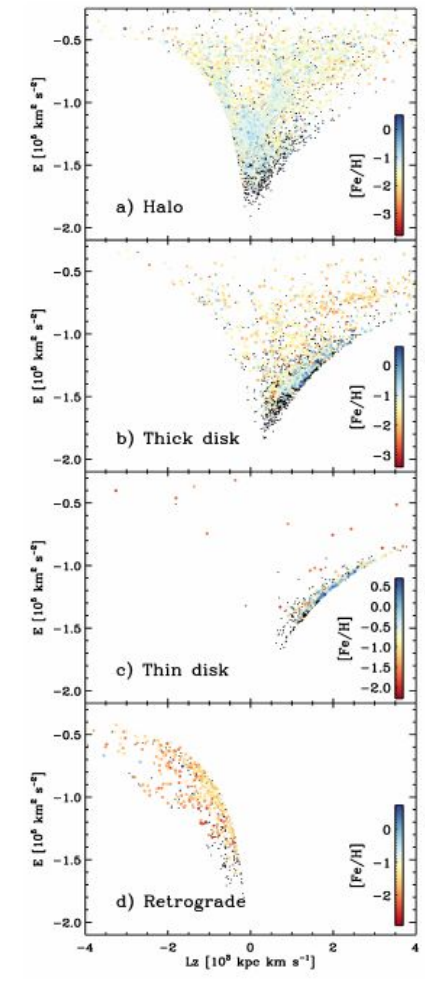
Metallicity

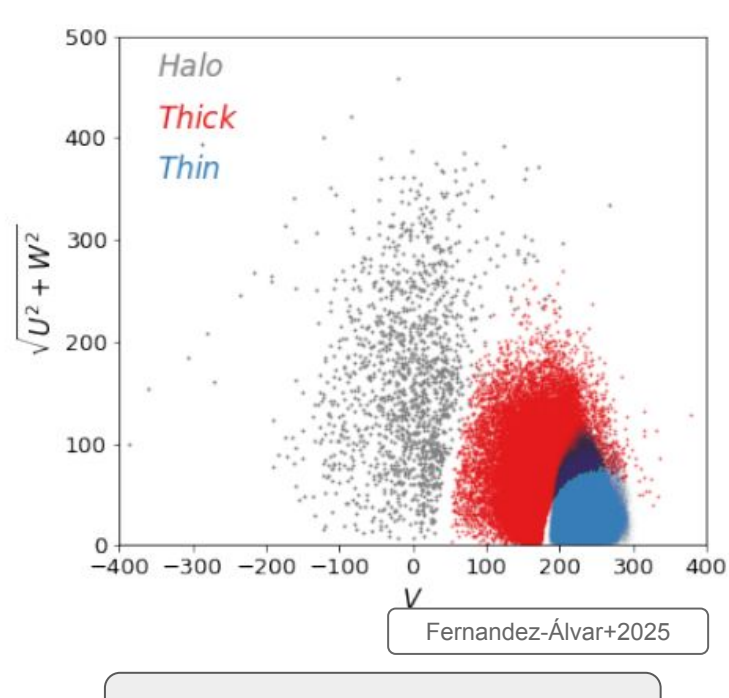
- similar distribution (peak)
- tails biassed by the samples

α-elements

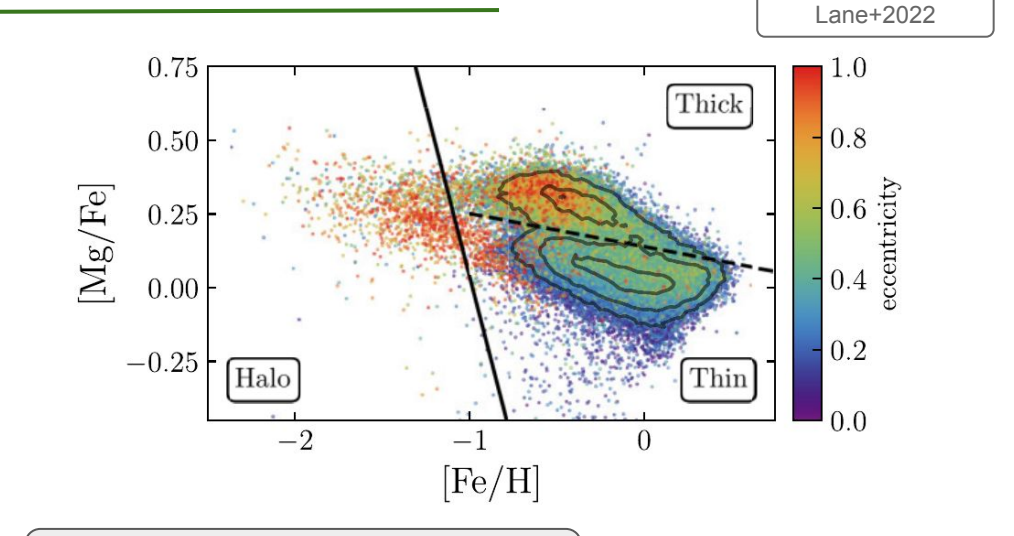
- Ca, Mg, Ti
- two peaks:
 - \circ α ~-0.04+/-0.01 dex σ =0.11+/-0.01 dex
 - \circ $\alpha \sim +0.32 + /-0.01 dex <math>\sigma = 0.19 + /-0.01 dex$

Dissecting the MW with RR Ly

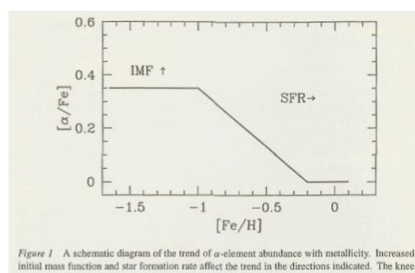




Kinematical definition



Chemical definition



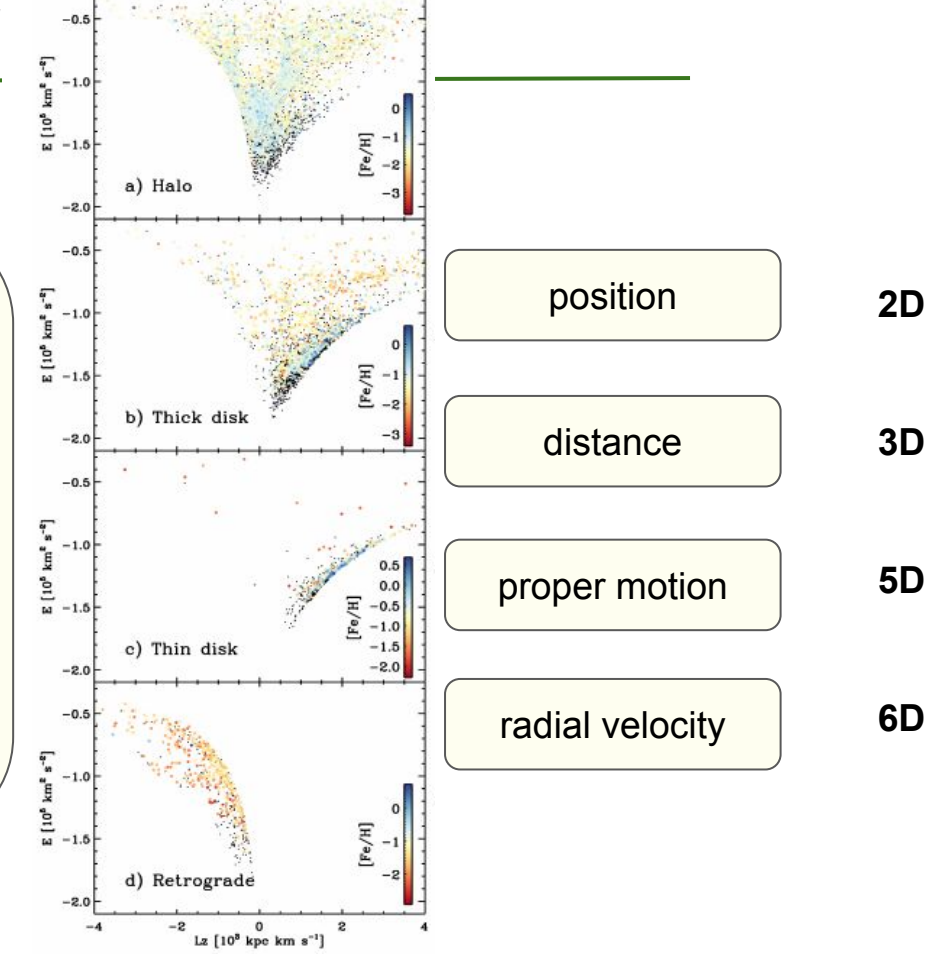
initial mass function and star formation rate affect the trend in the directions indicated. The knee

McWilliam 1997

Dissecting the MW with RR Ly

Assumptions:

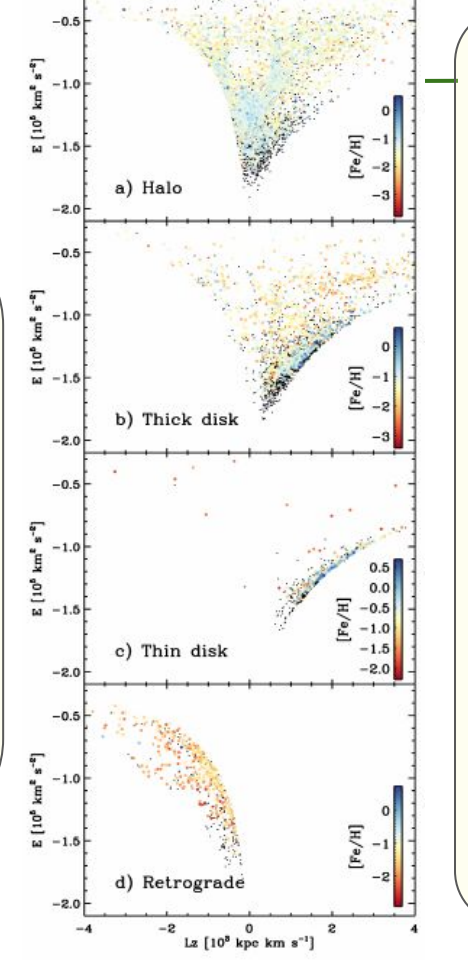
- Galactic potential
- Sun position
- Sun motion
- a code to reconstruct orbits (galpy, agama)
- distance to stars

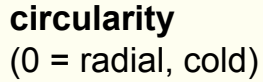


Dissecting the MW with RR Ly

Assumptions:

- Galactic potential
- Sun position
- Sun motion
- a code to reconstruct orbits (galpy, agama)
- distance to stars



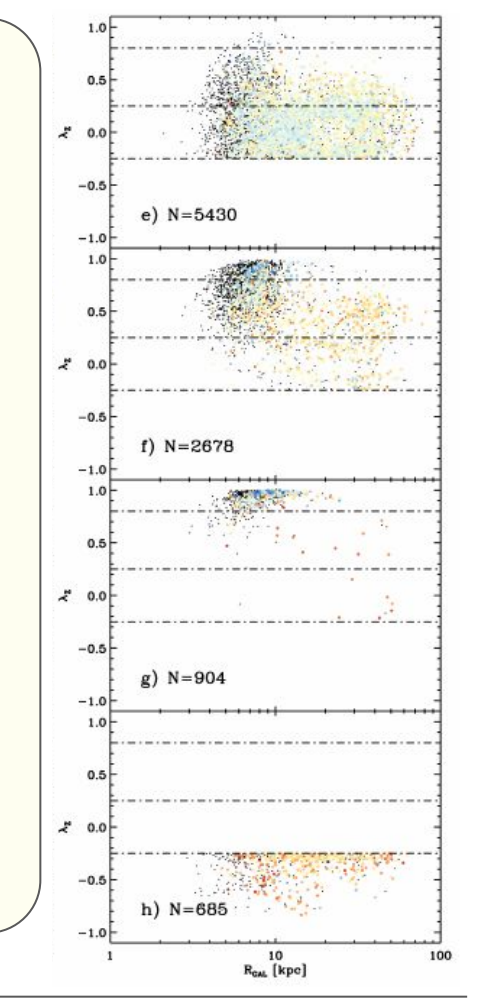


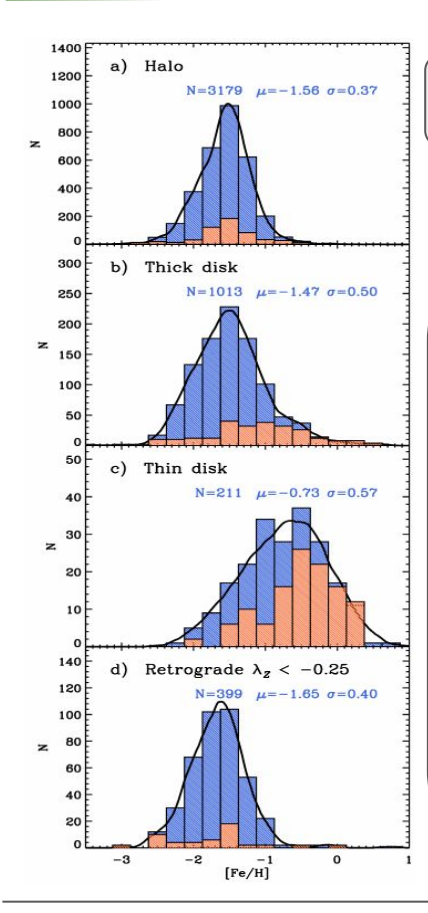
Halo: mostly cold, extend to large distances

Thick: warmer, more confined

Thin: mostly hot

Retrograde: confined in both parameters

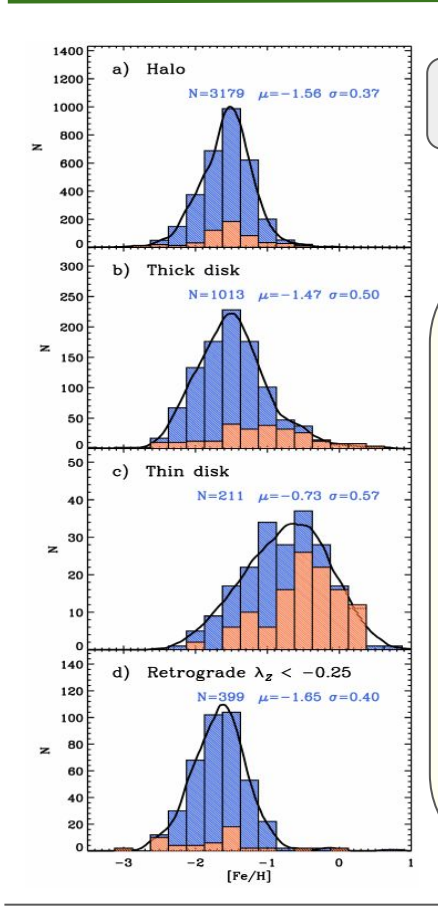




Chemical Characterization

Metallicity distribution:

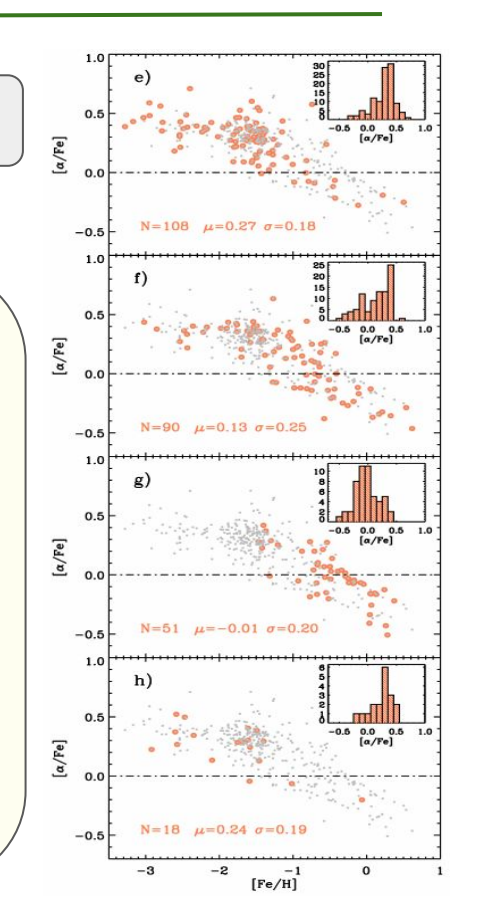
- ★ Peak shifts to higher metallicity halo → thick → thin
- **★ Dispersion** increases
- ★ Metal-rich tail in the thick disk
- ★ Retrograde ~ halo



Chemical Characterization

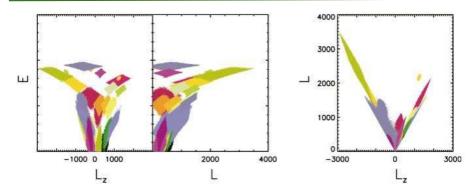
Metallicity distribution:

- ★ Peak shifts to higher metallicity halo → thick → thin
- **★ Dispersion** increases
- ★ Metal-rich tail in the thick disk
- ★ Retrograde ~ halo



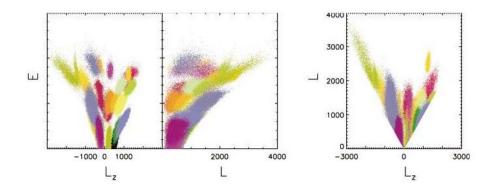
α-elements:

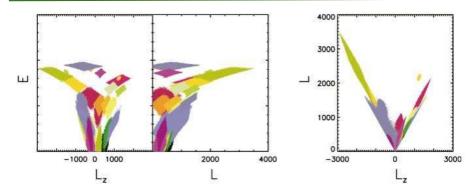
- ★ halo: α-enhanced [α/Fe]~0.27 and metal poor
- thick: α-enhanced and metal poor or α-poor and metal-rich
- thin: mainly α-poor/depleted
- ★ Retrograde ~ halo



Helmi+1999,2000

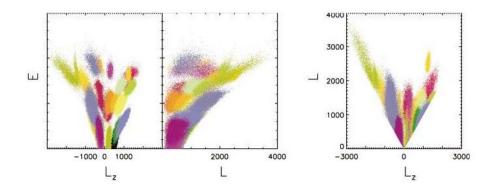
Figure 3. Initial distribution of particles in the integrals of motion space. The different colours represent different satellites.

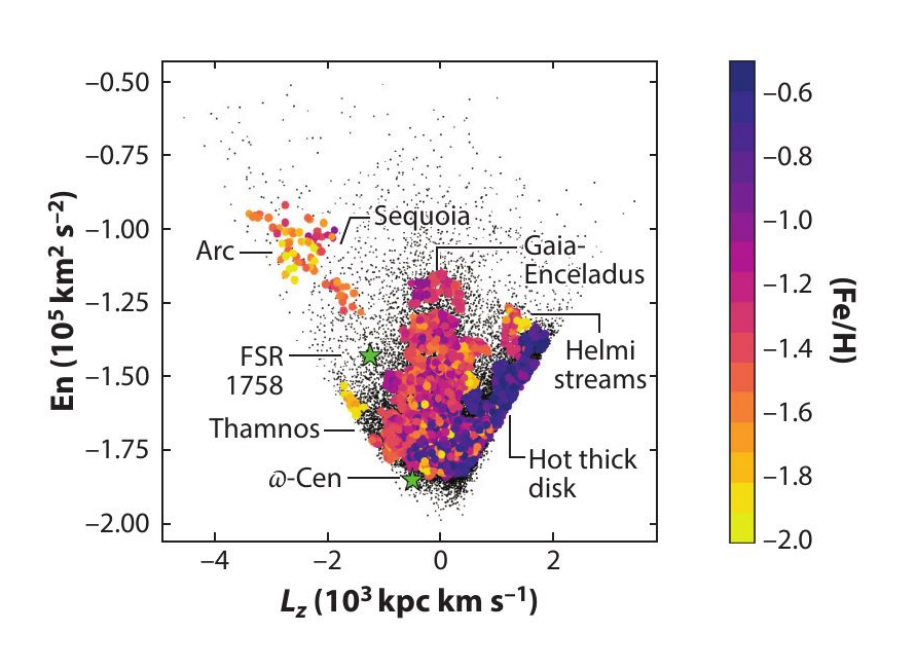




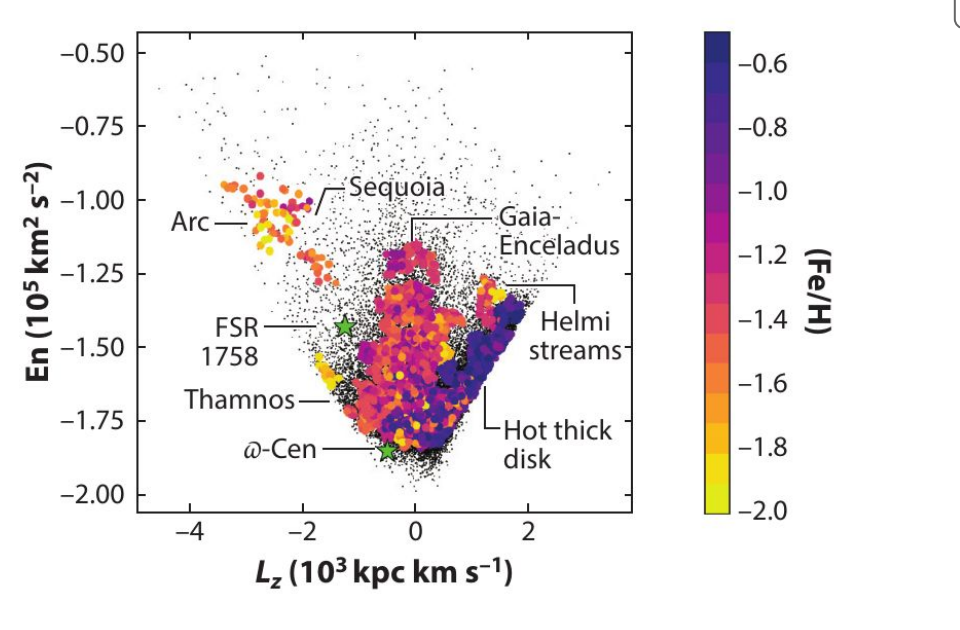
Helmi+1999,2000

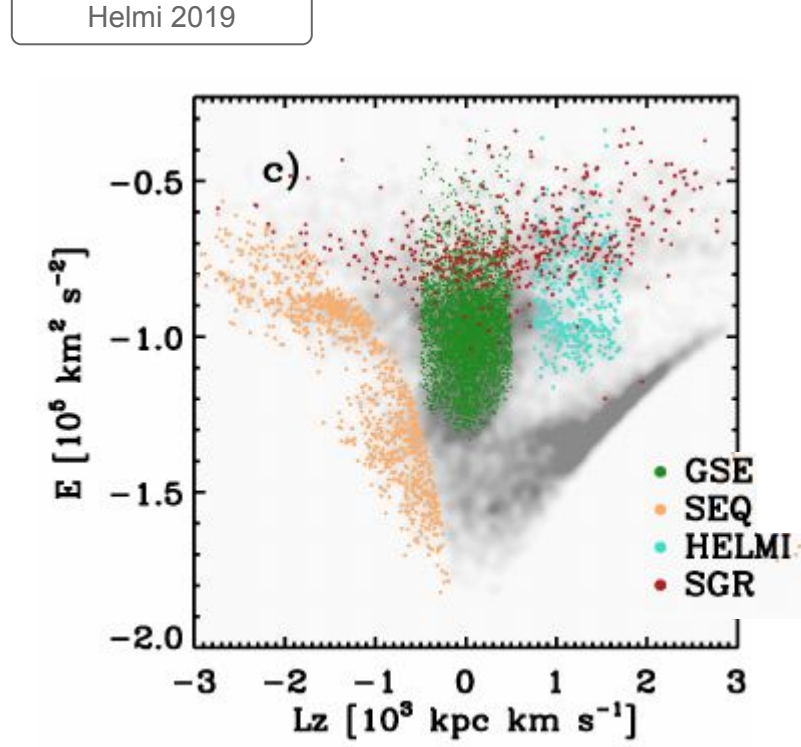
Figure 3. Initial distribution of particles in the integrals of motion space. The different colours represent different satellites.



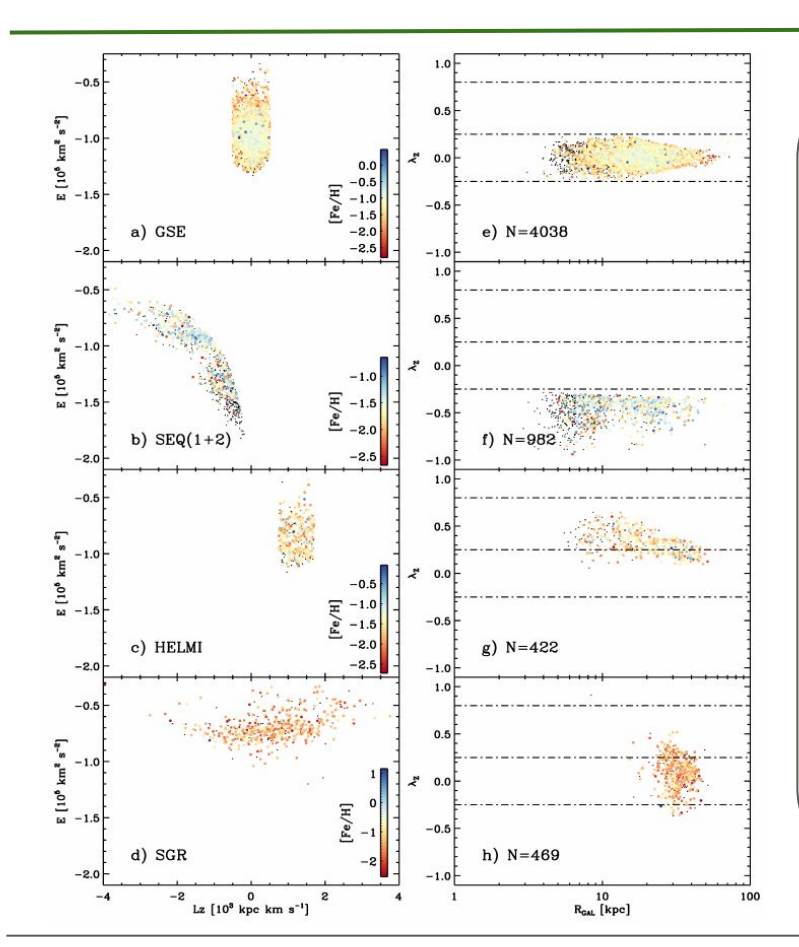


Helmi 2019





Dissecting the MW with RR Lyrae stars

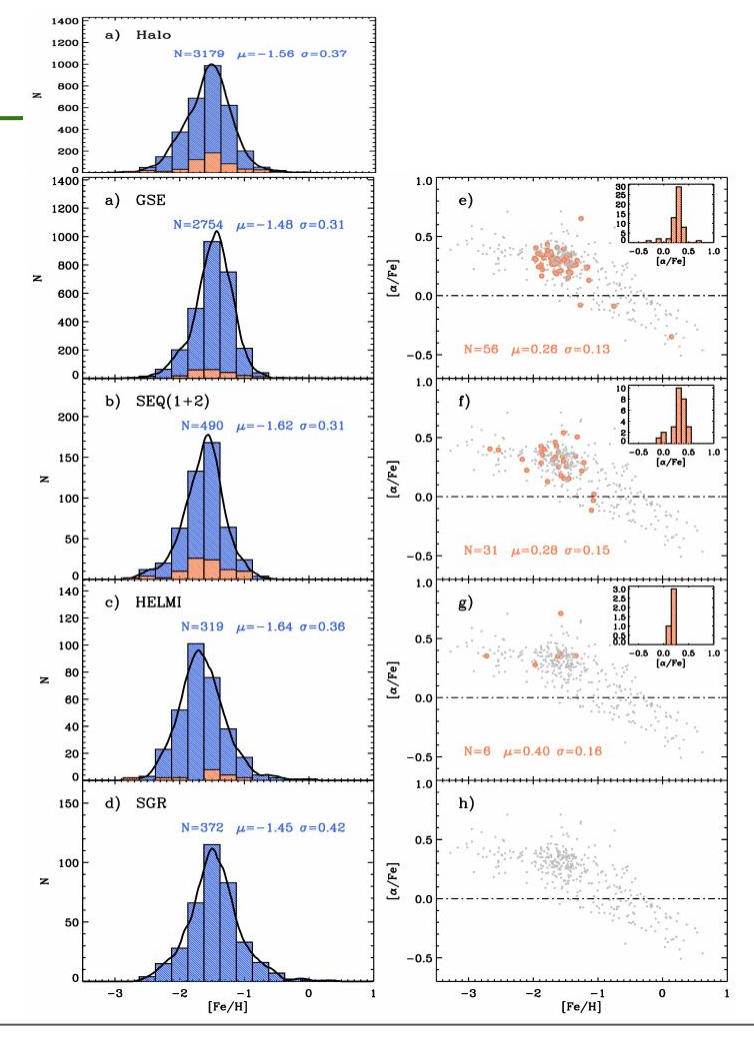


- ★ GES: homogeneous both in metallicity and and orbital energy over a wide range of distances
- ★ Sequoia: more confined and metal-rich, retrograde
- ★ Helmi: hints of metallicity gradient

★ Sagittarius: more metal poor, radial orbits

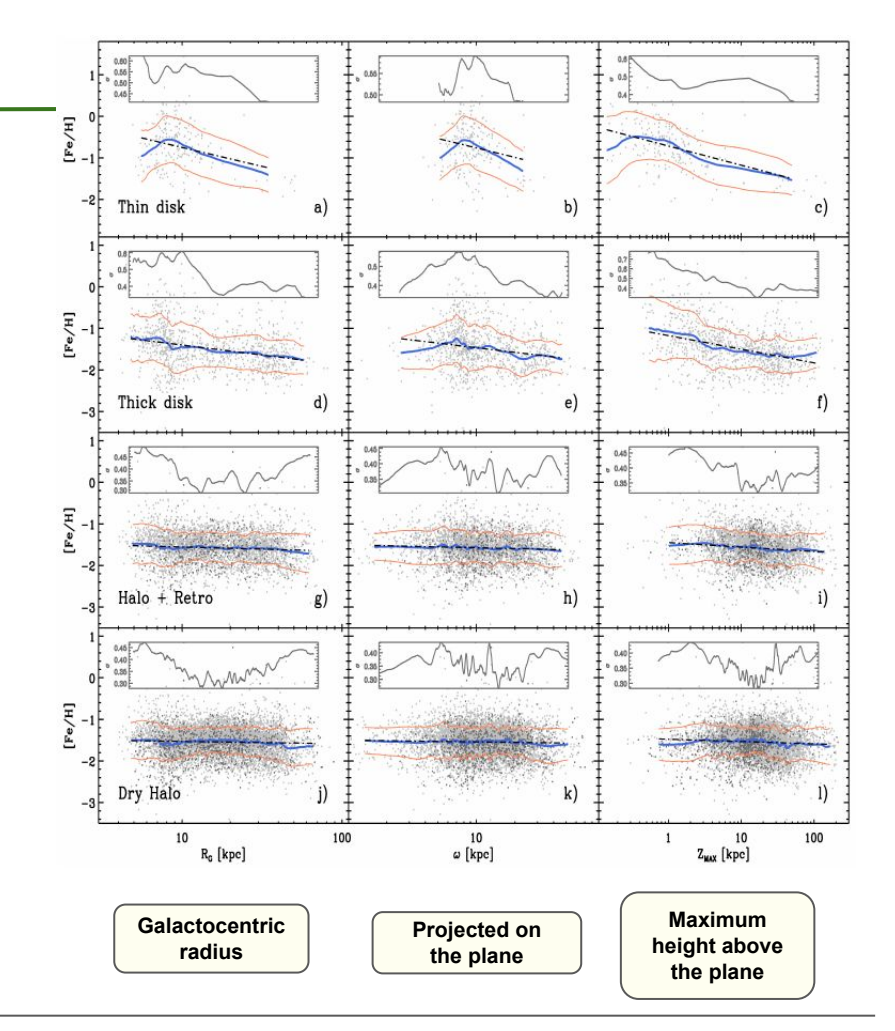
Dissecting the MW with RR Lyrae stars

- ★ overall large similarities with the halo sample
- ★ mild dispersion variations
- * small samples with α-abundances
 - → a lot to be done!
 Gaia DR4 +
 spectroscopic surveys

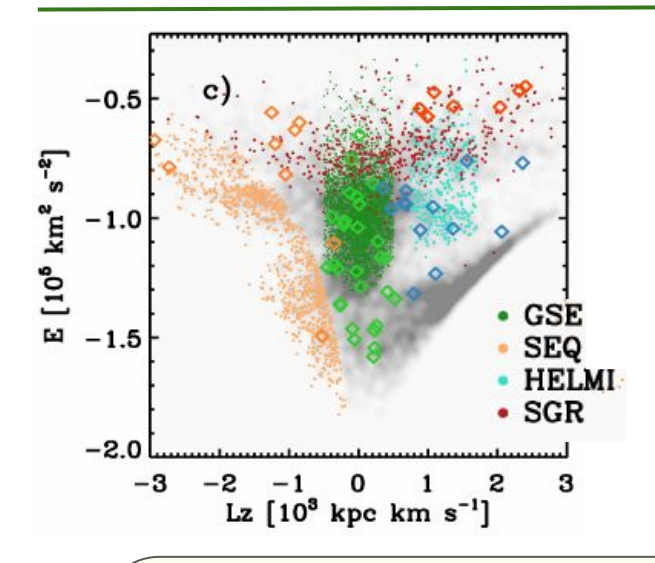


Metallicity gradients

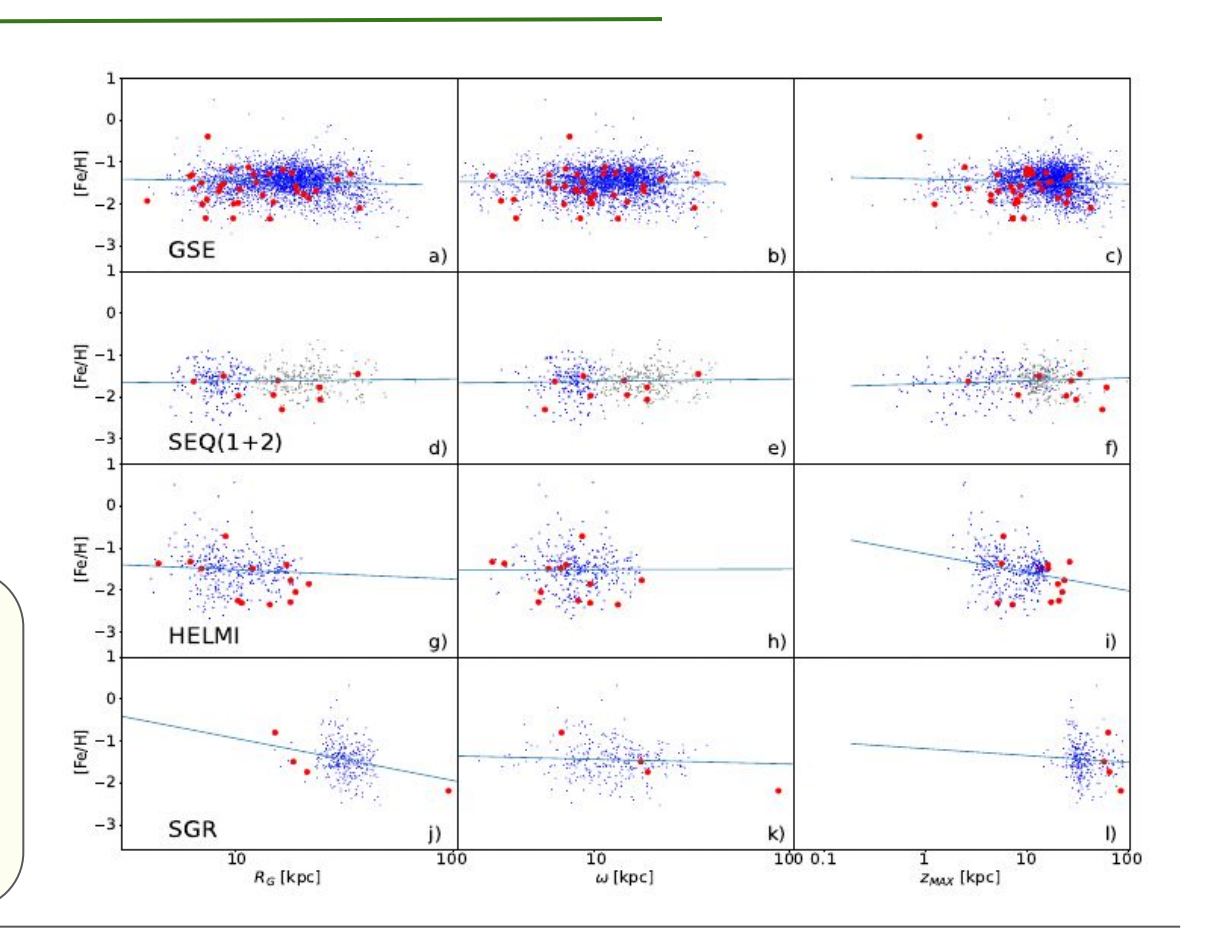
- ★ Thin: limited distance but steeper gradient
- ★ Thick: well defined radial gradient; increase of dispersion at the solar circle
- ★ Halo+retro: mild gradient and large dispersion over a large distance range
- ★ **Dry halo**: no stars from streams.



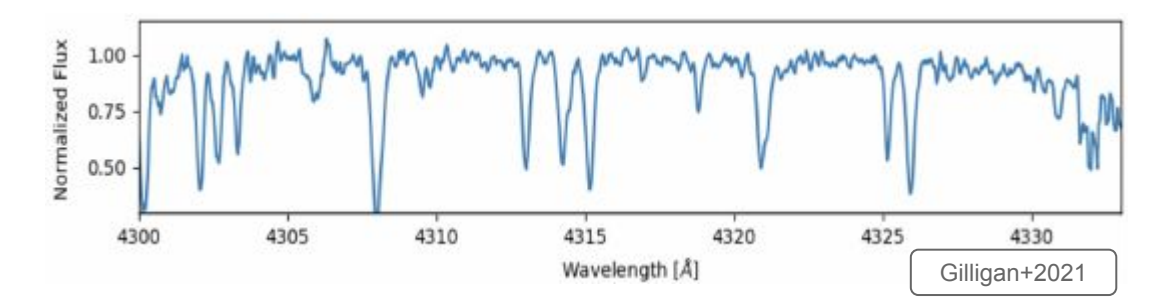
Metallicity gradients



- ★ Overall good agreement between field and GCs stars
- ★ **GES**: flat + constant dispersion. Good agreemnt with GCs.
- ★ Sequoia: differentiation between Seq. 1 and 2

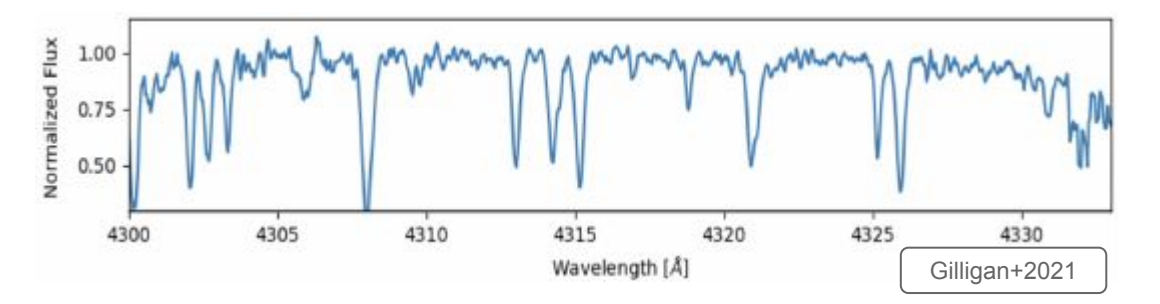


High Resolution



- \star R > 20,000
- ★ fundamental parameter determination
- ★ line/spectral synthesis
- ★ errors in [Fe/H] ~ 0.2 dex
- tricky business!
- doppler shift, line deformation, P Cygni profile, shocks
- ♦ high S/N in a short time
- slow process

High Resolution



- \star R > 20,000
- ★ fundamental parameter determination
- ★ line/spectral synthesis
- ★ errors in [Fe/H] ~ 0.2 dex
- tricky business!
- doppler shift, line deformation, P Cygni profile, shocks
- ♦ high S/N in a short time
- slow process

Radial velocity:

< 3000 *

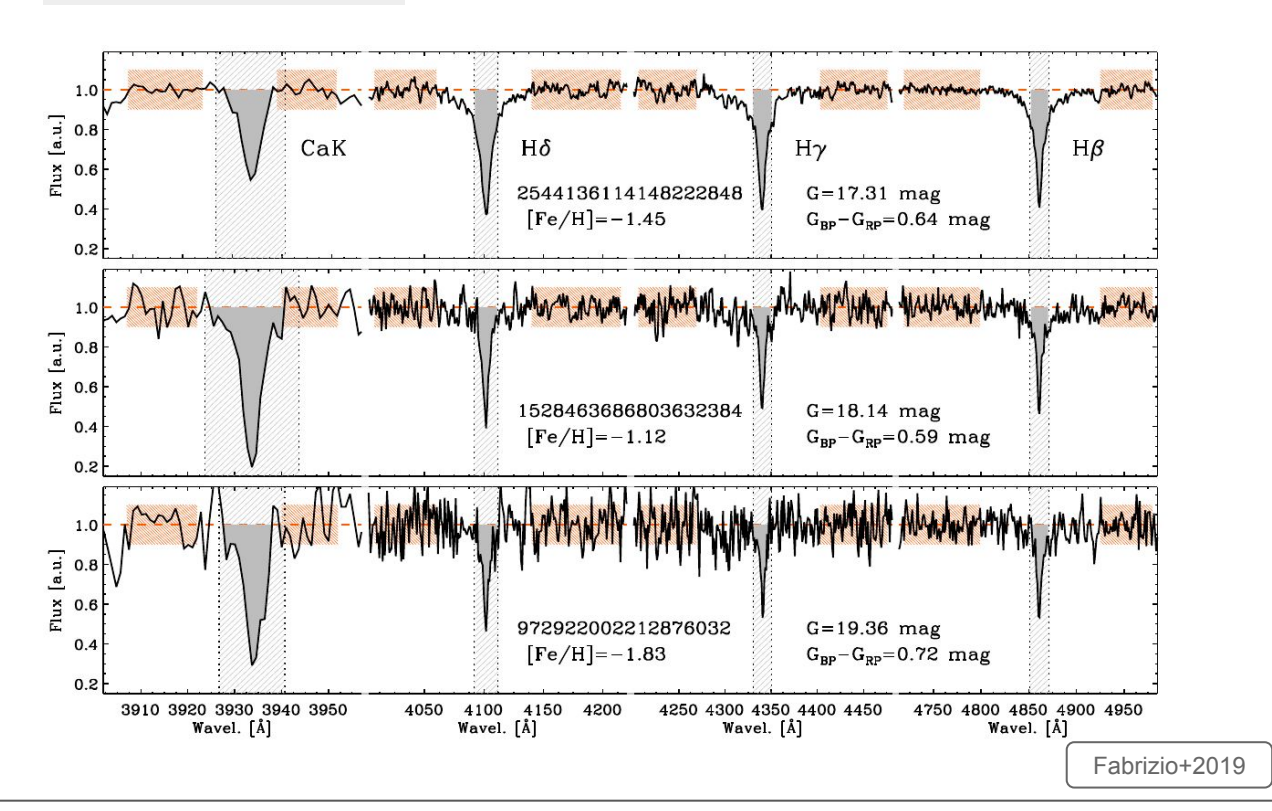
Metallicity:

< 400 *

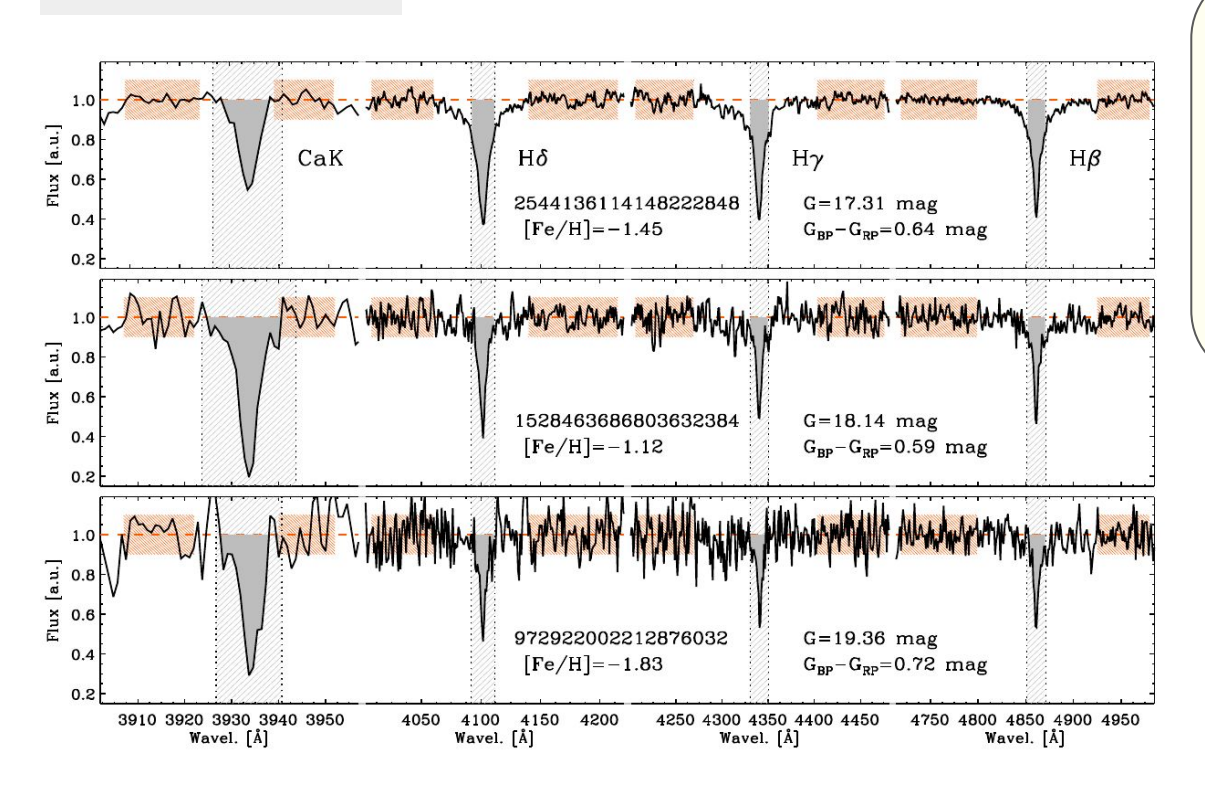
- → 4MOST
- → WEAVE

thousands of RRL stars

Low Resolution



Low Resolution



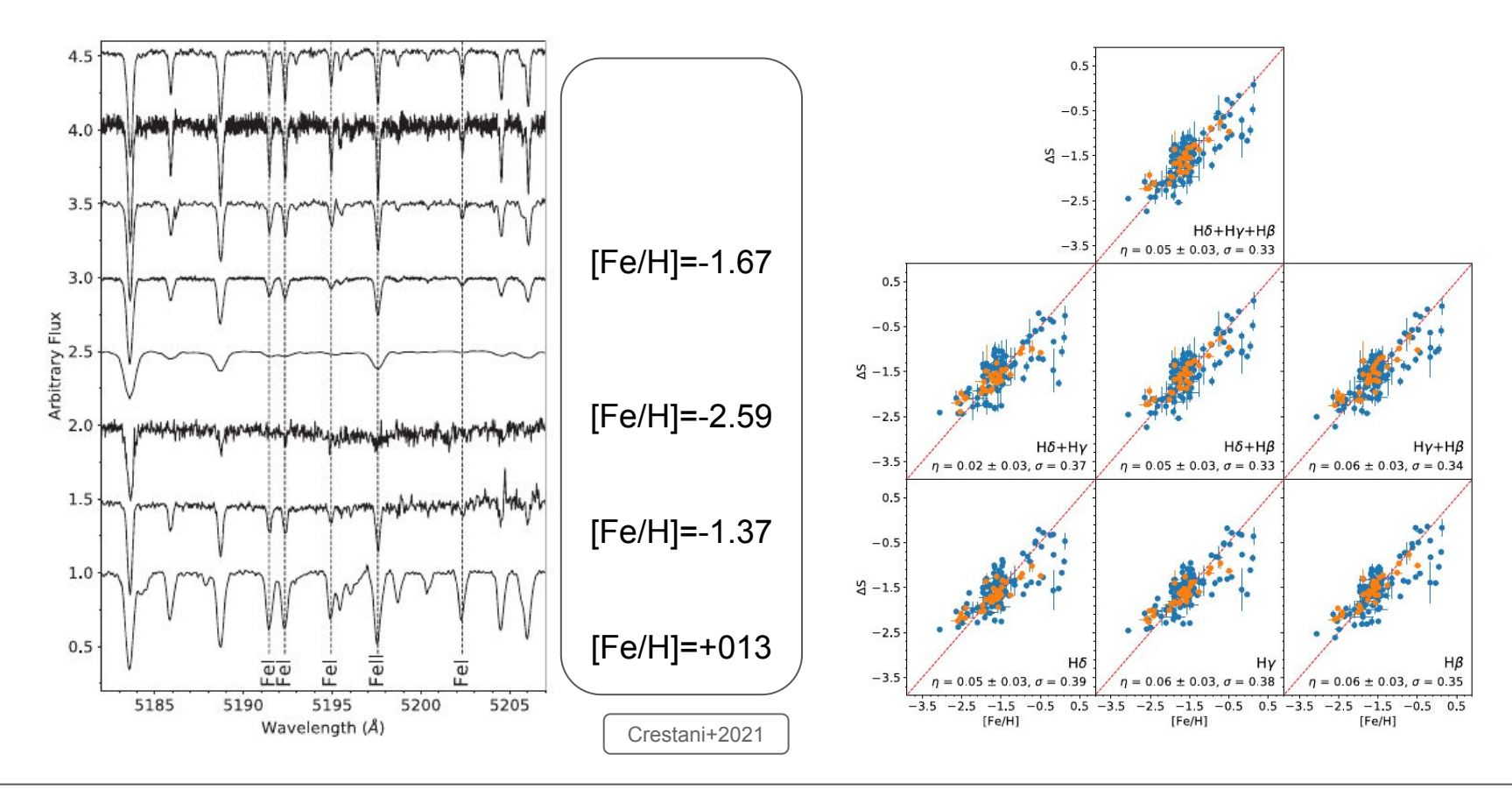
- \star R > 2,000
- ★ Preston (1959) difference in equivalent width of Ca II Kline and Balmer lines
- ★ more efficient
- ★ less precise ~0.3-0.4 dex
- ★ Crestani+2021 calibration on 143 stars with HR

Radial velocity:

~13000 *

Metallicity:

< 8000 *



The pulsational properties are connected to the chemistry of the star

Different relations have been proposed to infer the metallicity of the RRL star from its light curve properties, correlating [Fe/H] with

- the Fourier parameters (Jurcsik & Kovacs 1996, Nemec 2013)
- the period (Sarajedini 2006)
- the period and the amplitude (Alcock+2000)
- the period and the amplitude (theoretical, Bono+2007)
- the period and the luminosity (Braga+2016)

Metallicity of RR Lyrae stars: Photometry

Fourier coefficients

★ Jurcsik & Kovacs (1996) first find a linear relation between [Fe/H], the period and the Fourier coefficients

$$m(\phi) = A_0 + \sum_{i=1}^n A_i \sin[2\pi i(\phi + \phi_0) + \phi_i]$$

★ Certain coefficients correlate with metallicity

$$\Phi_{31} = \Phi_3 - 3\Phi_1$$

★ different relations in different filter passbands: V, G (Gaia), Kp (Kepler), I (OGLE), mid IR Radial velocity:

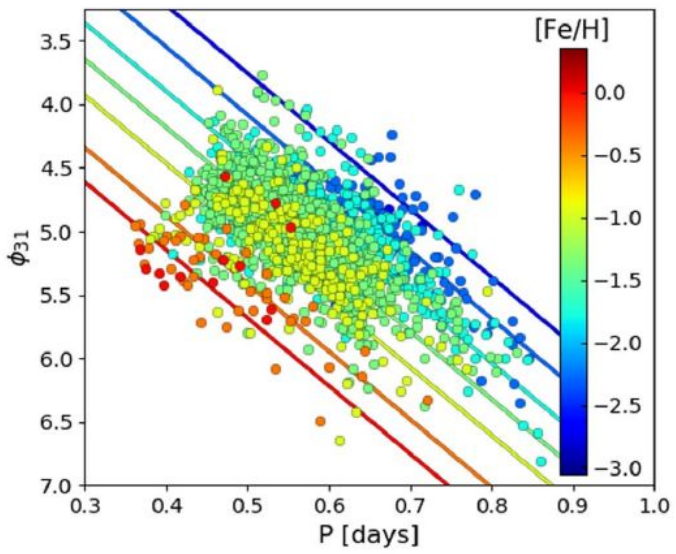
~13000 *

Metallicity:

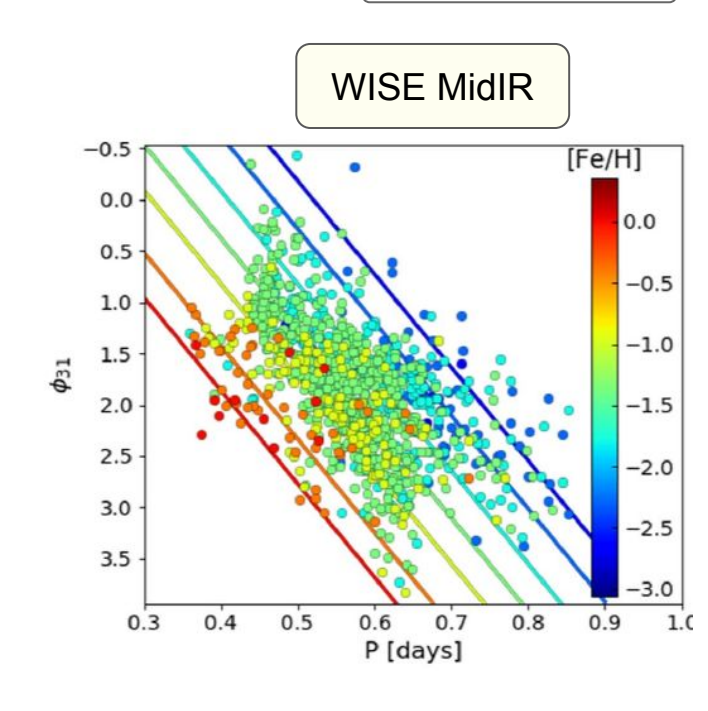
< 8000 *

Mullen+2021,2022

Fourier coefficients ASAS-SN V



[Fe/H] =
$$(-1.22 \pm 0.01) + (-7.60 \pm 0.24) \cdot (P - 0.58) + (1.42 \pm 0.05) \cdot (\phi_{31} - 5.25)$$
; rms = 0.41,

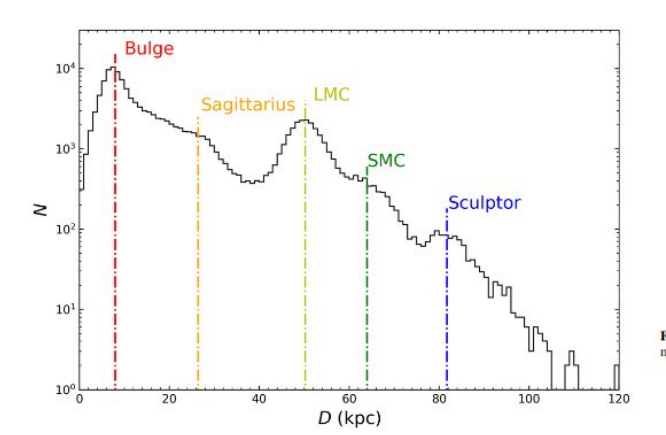


[Fe/H] =
$$(-1.47 \pm 0.02) + (-8.33 \pm 0.34) \cdot (P - 0.58) + (0.92 \pm 0.05) \cdot (\phi_{31} - 1.90)$$
; rms = 0.50.

Metallicity of RR Lyrae stars: Photometry

 Hajdu+2018, Dekany+2018,2021, 2022: application to OGLE and VVV

 Li+2023: recalibration of the Fourier-metallicity relation, based on ~5,000 LAMOST star (low-res); metallicity and distances of 136,000 RRL



[Fe/H] =
$$a_0 + a_1(P - 0.6) + a_2(\phi_{31} - 2) + a_3(R_{21} - 0.45),$$

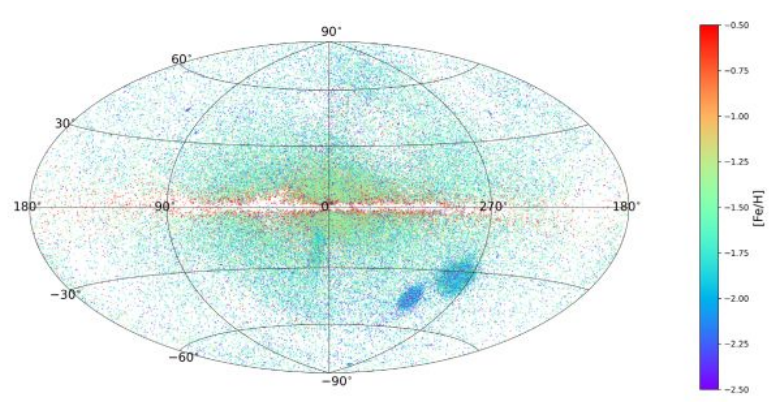


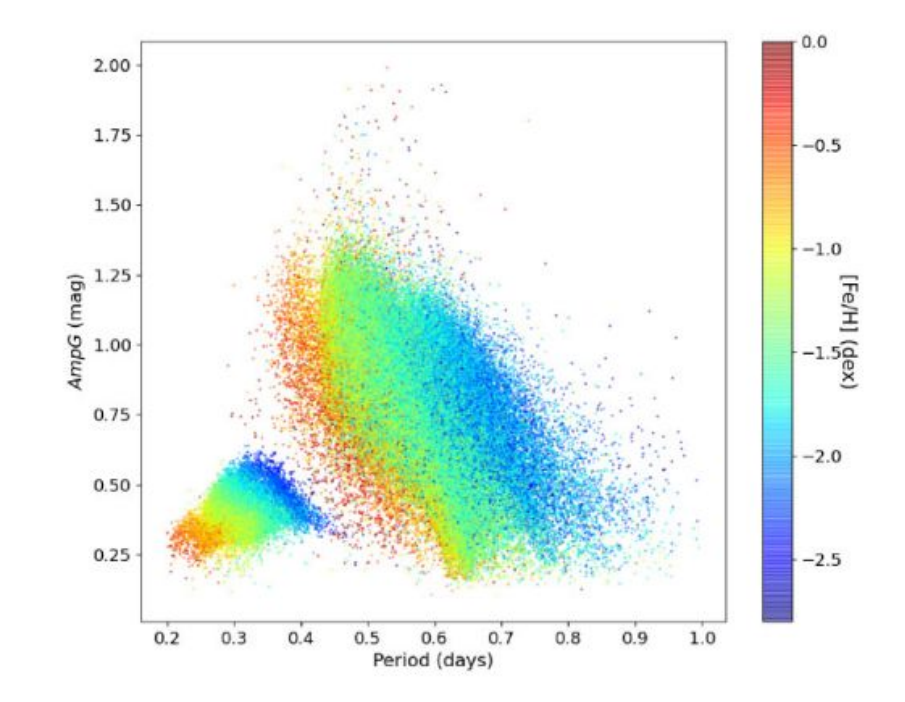
Figure 5. The sky distribution of our final RRL sample of 135,873 RRLs (115,410 type RRab and 20,463 type RRc stars) in Galactic coordinates, color-coded by metallicity, as shown in the color bar.

Metallicity of RR Lyrae stars: Photometry

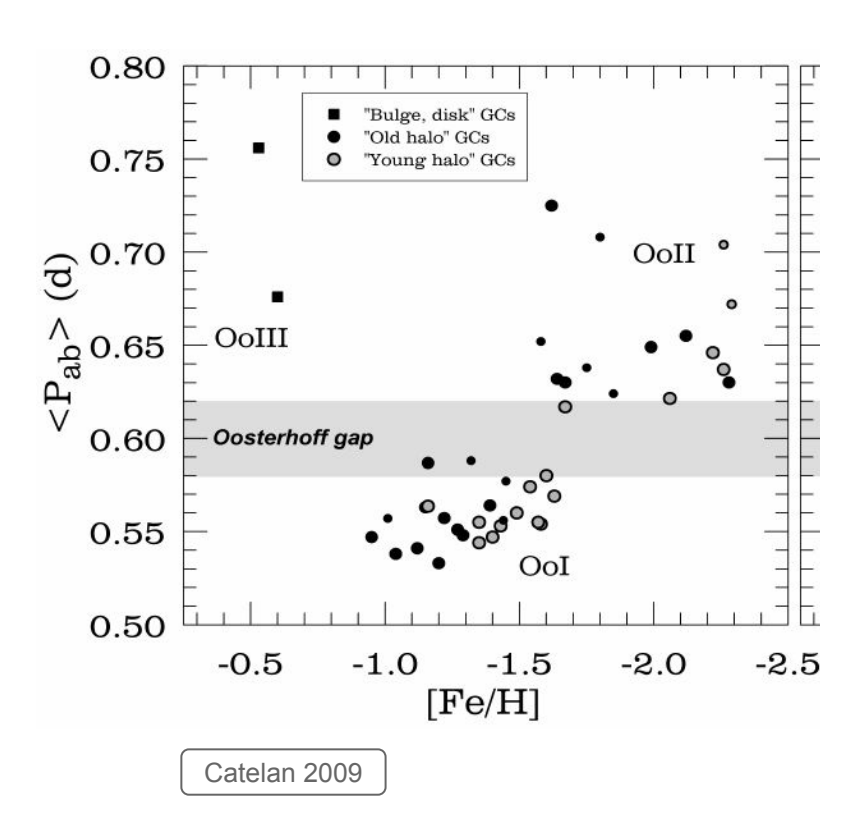
- Hajdu+2018, Dekany+2018,2021, 2022: application to OGLE and VVV
- Li+2023: recalibration of the Fourier-metallicity relation, based on ~5,000 LAMOST star (low-res); metallicity and distances of 136,000 RRL
- Muraveva+2025; 134,000

[Fe/H] =
$$(-8.54 \pm 0.42)P + (0.23 \pm 0.04)\phi_{31}$$

- $(9.34 \pm 1.41)A_2 + (0.80 \pm 0.19)$.



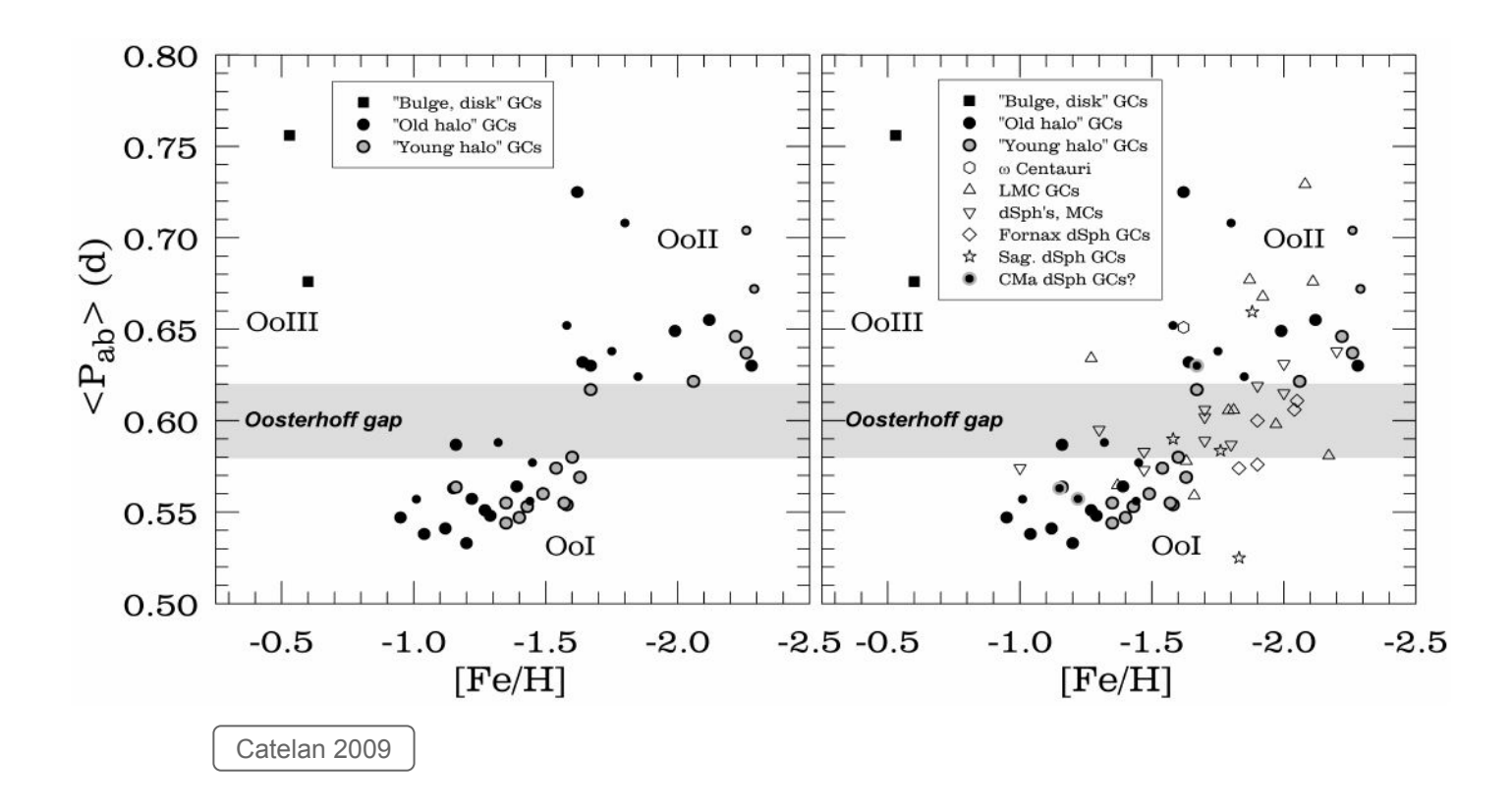
On the Oosterhoff dichotomy



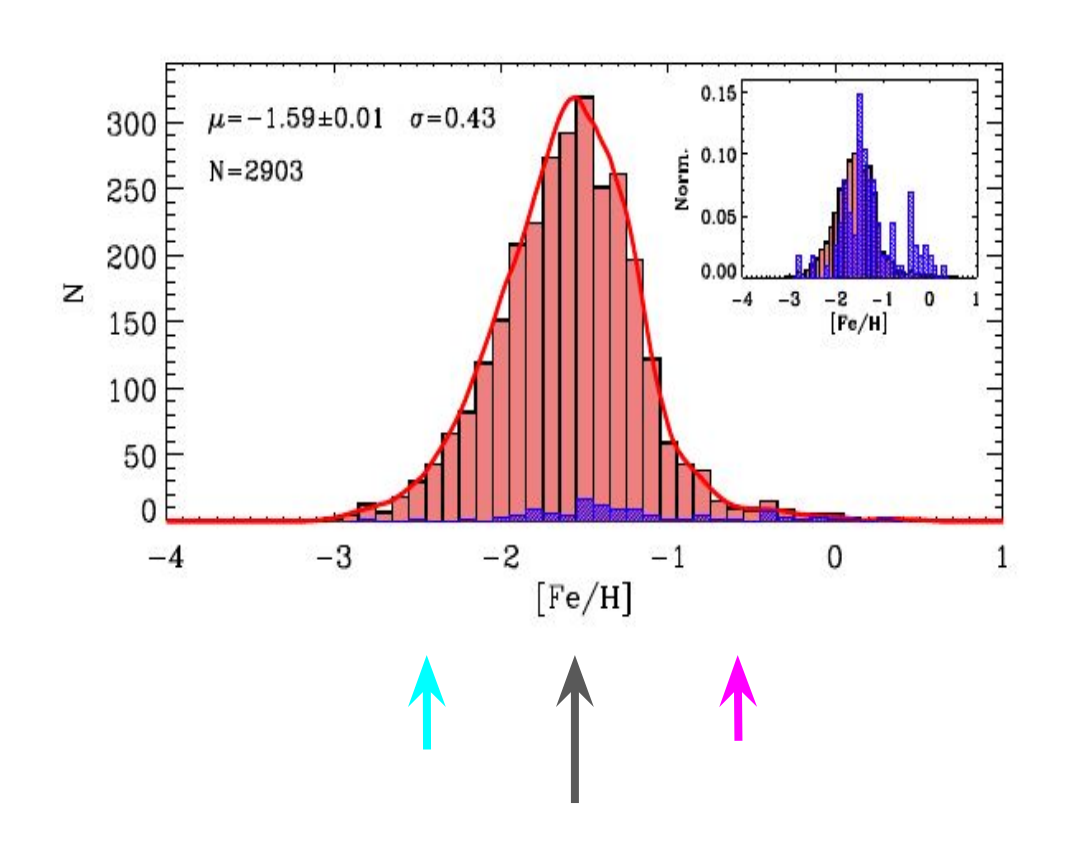
| , | c-type. | | | a- and b -type. | | |
|-------|----------|--------------------|-----------------|-------------------|-------------------|----------------|
| | Number. | Median period. | Mean period. | Number. | Median period. | Mean period |
| | | d | d | | d | d |
| ω Cen | 57 | ·38' ·38 ·38 | *37 | 77 | ·63 | .65 |
| М 15 | 57 28 | -38 | :38 | 31 | ·66 | ·65 |
| M 53 | 15 | •38 | .36 | 17 | .62 | .62 |
| М 5 | 13 | •32 | .32 | 63 | .54 | .54 |
| М 3 | 27 | .32 | .32 | 124 | .54 | .55 |

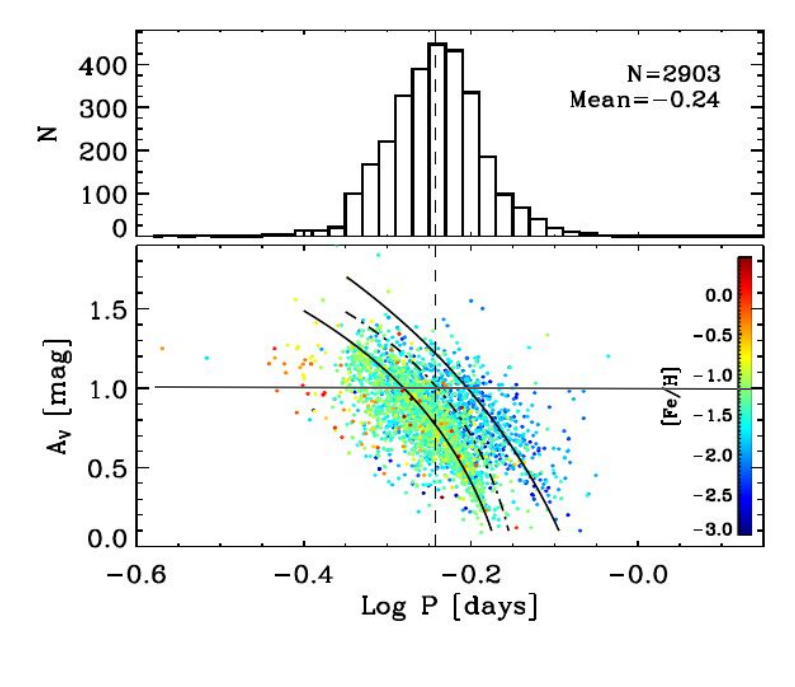
Oosterhoff 1939

On the Oosterhoff dichotomy





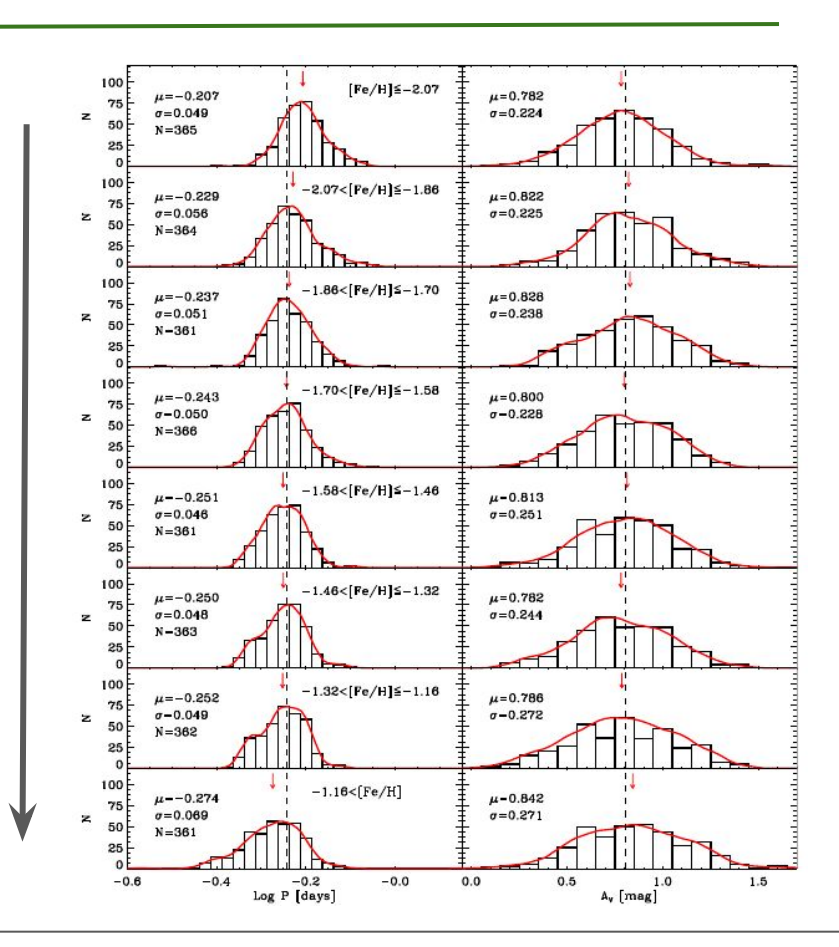




Fabrizio+2019

- ★ the mean period decreases for increasing metallicity
- ★ asymmetric distribution
- ★ skewness moves from the metal-rich to the metal-poor tail for increasing metallicity

metallicity



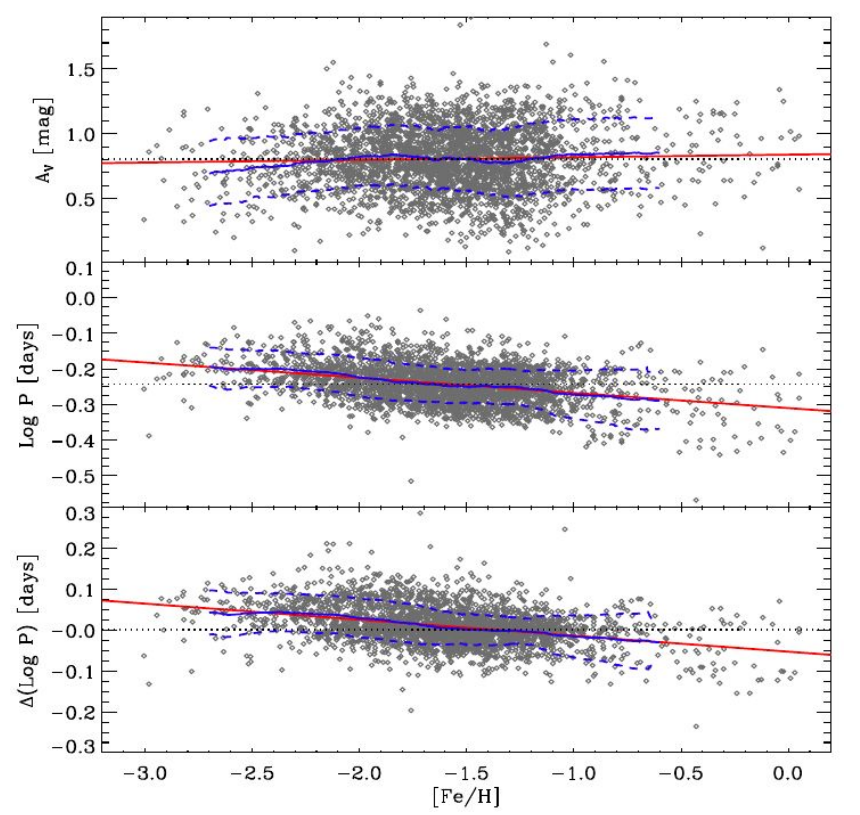
Fabrizio+2019

- ★ the mean period decreases for increasing metallicity
- ★ asymmetric distribution
- ★ skewness moves from the metal-rich to the metal-poor tail for increasing metallicity

[Fe/H]≤-2.07 $\mu = -0.207$ $\mu = 0.782$ $\sigma = 0.049$ $\sigma = 0.224$ N=365 100 -2.07<[Fe/H]≦-1.86 $\mu = -0.229$ $\mu = 0.822$ $\sigma = 0.056$ $\sigma = 0.225$ N=364 100 -1.86<[Fe/H]≤-1.70 $\mu = -0.237$ $\mu = 0.828$ $\sigma = 0.051$ a = 0.238N-361 100 -1.70<[Fe/H]≦-1.58 $\mu = -0.243$ $\mu = 0.800$ $\sigma = 0.050$ $\sigma = 0.228$ 50 N=366 25 100 -1.58<[Fe/H]≤-1.46 $\mu = -0.251$ $\mu = 0.813$ $\sigma = 0.046$ $\sigma = 0.251$ N=361 25 100 -1.46<[Fe/H]≤-1.32 $\mu = -0.250$ $\mu = 0.782$ $\sigma = 0.048$ $\sigma = 0.244$ 50 N-363 100 -1.32<[Fe/H]≦-1.16 $\mu = -0.252$ $\mu = 0.786$ $\sigma = 0.049$ $\sigma = 0.272$ N=362 25 100 -1.16<[Fe/H] $\mu = -0.274$ $\mu = 0.842$ $\sigma = 0.069$ $\sigma = 0.271$ 50 N=361 -0.6-0.4-0.2 -0.00.0 0.5 1.5 Log P [days] A_v [mag]

★ not so clear trend for the amplitude

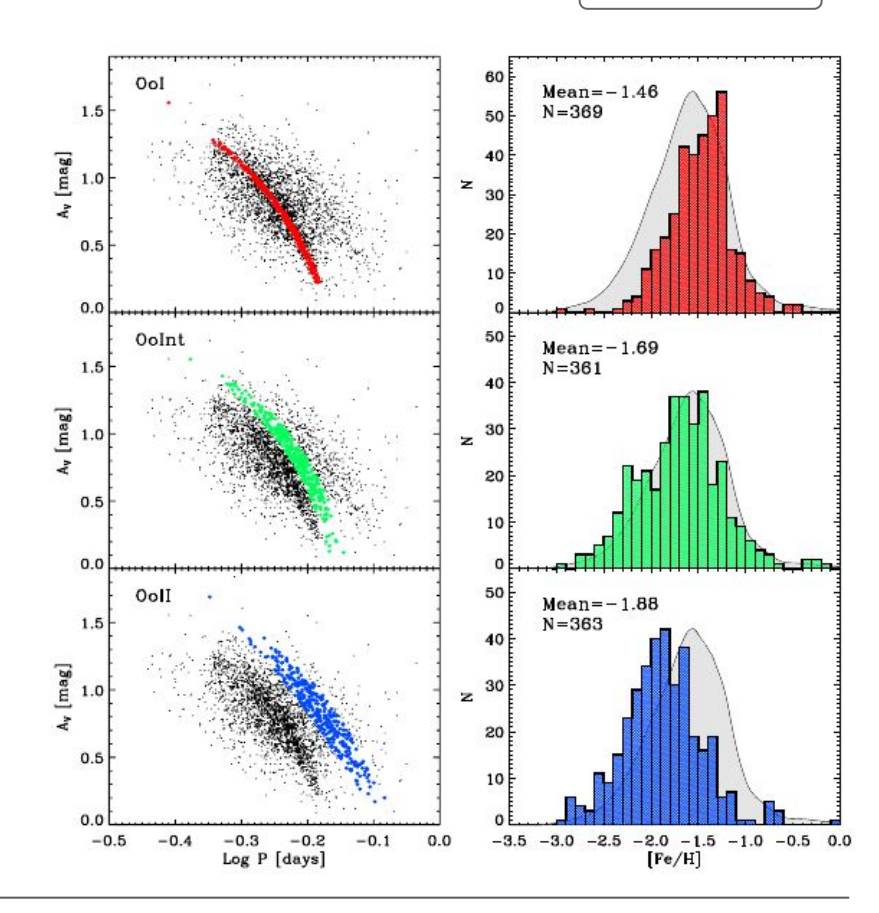
metallicity



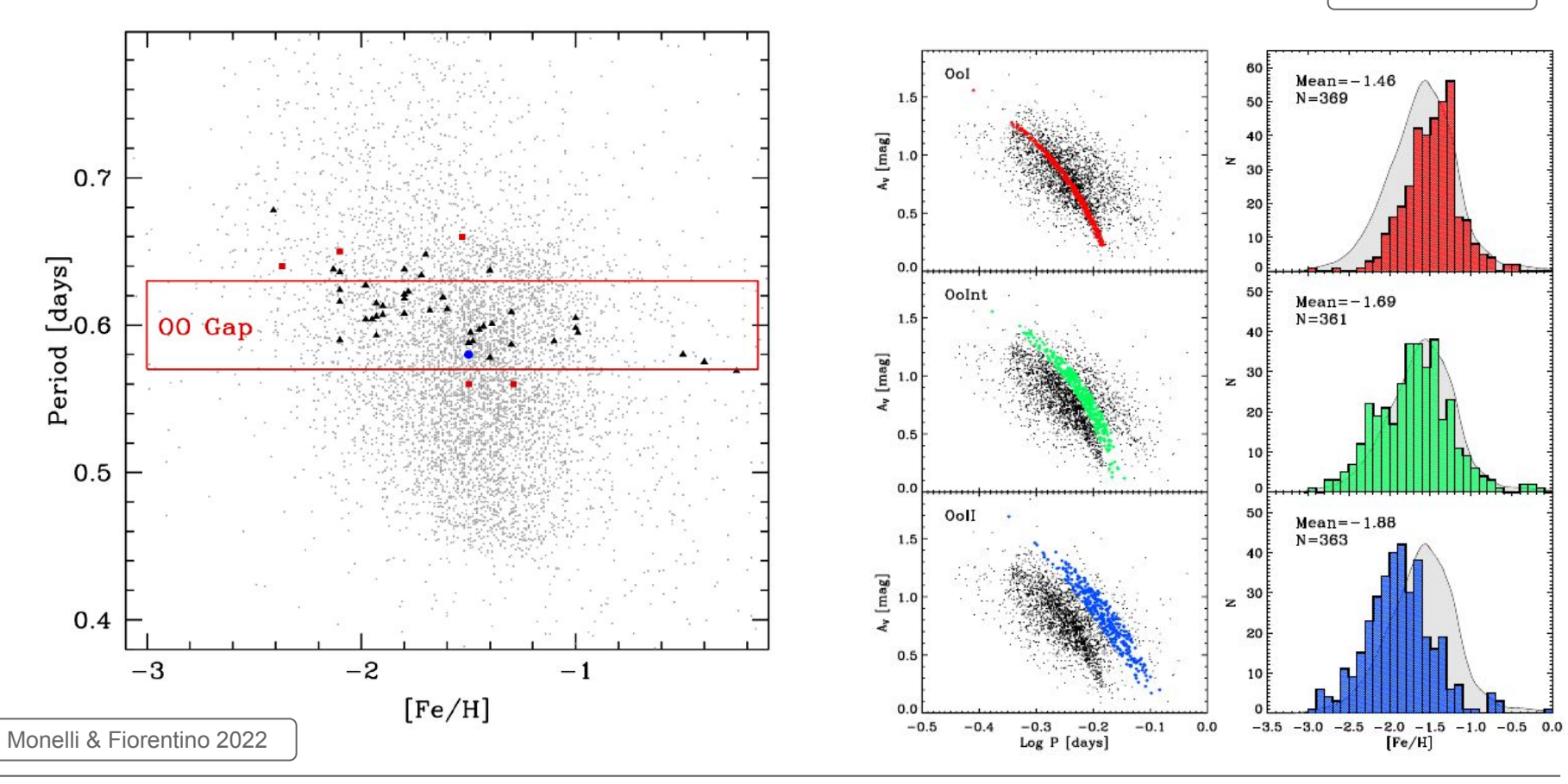
$$A_V = 0.84(\pm 0.02) + 0.02(\pm 0.01) \cdot [\text{Fe/H}].$$

$$\log P = -0.311(\pm 0.004) - 0.044(\pm 0.002) \cdot [\text{Fe/H}].$$

$$\Delta \log P = -0.054(\pm 0.003) - 0.040(\pm 0.002) \cdot [\text{Fe/H}].$$

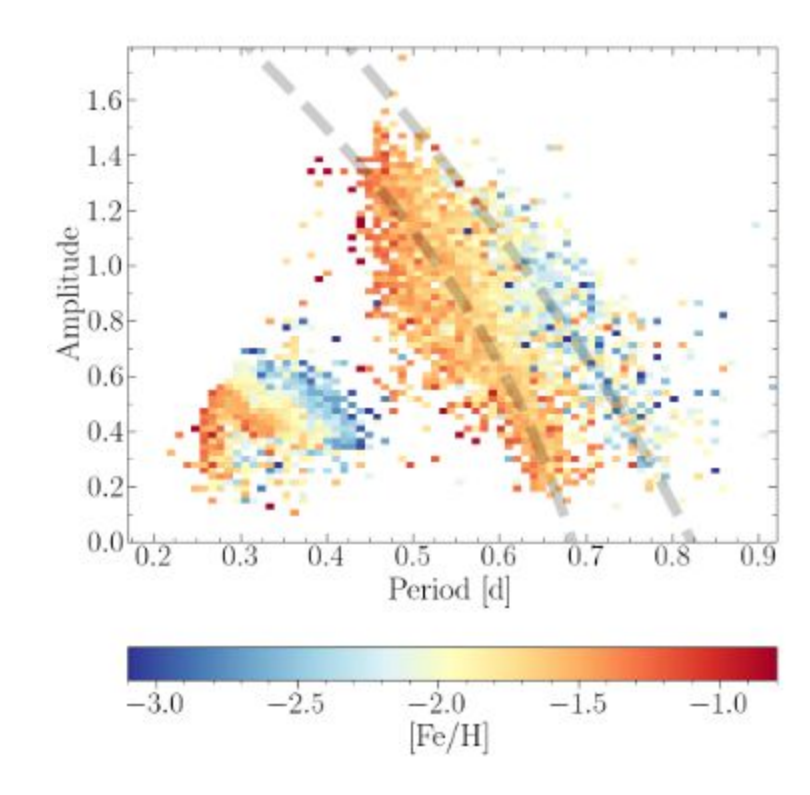


Fabrizio+2019



Medina+2025abc

★ DESI DR1★ 6420 RRL★ R~2,500



Medina+2025abc

